አዳማ ሳይንስ እና ቴክኖሎጂ ዩኒቨርሲቲ

Adama Science & Technology University

SCHOOL OF ELECTRICAL ENGINEERING AND COMPUTING

DEPARTMENT OF ELECTRONICS & COMMUNICATION ENGINEERING

DVB-T2 GUARD INTERVAL OPTIMIZATION for SFN (Case Study on OTV)

Prepared by Yusuf Jamaal

A Thesis Submitted in Partial Fulfillment of the Requirements
For the Award of the
Degree of Master of Engineering (Communication System Engineering)

Adama, Ethiopia June 2017

DVB-T2 GUARD INTERVAL OPTIMIZATION for SFN

(Case Study on OTV)

Submitted by:

Yusuf Jamaal	________________	________________
Student	Signature	Date

Approved by:

Dr. Sultan Feisso	________________	________________
Advisor	Signature	Date
Internal Examiner:	________________	________________
Dr. M.Venkata Raghuvandra	Signature	Date
External Examiner:	________________	________________
Dr. Eristu Yigzaw	Signature	Date
Chairman, Department:	________________	________________
Eng. Hinsermu Alemayehu	Signature	Date

School Dean:

____________________	________________	________________
	Signature	Date

Abstract

Oromia Radio and TV Organization have launched analog terrestrial TV transmitters in different zonal parts of Oromia in 2008. All these transmitters broadcast analog signal in VHF frequency and MFN. These analog TV signals experience different distortions (ghosting) at receiving end from delayed (echoed) signal caused by different structures, buildings, wind farms and remote transmitter operating at the same frequency (co-channel).

To identify distortions caused by multipath reflections and co-channel overlaps we have tested the pure generated RF signal at the Lab by generating 10MHz RF from Agilent Spectrum analyzer, the transmitted or reference monitor out signal from OTV transmitters found at Adama, Kechema site and Sabata, Furi site. These two transmitters operate at the same frequency and all of their parameters are the same.

We have also measured the received input voltage at multipath environment i.e. Adama city at different places in which we have thought multipath reflections is high by using dipole antenna, DS1191 analyzer and TV set. We have got fluctuating input voltage at one place on our DS1191 and ghosted image on our TV set.

For co-channel overlap environment i.e. Bishoftu city we have made measurements and OTV signal from the two transmitters are reaching the receiver and we have got two spectrums on our DS1191 analyzer and fluctuating input voltages at a place.

We have also calculated the required ideal received input power/voltage at receiver by using Friis transmission calculator formula by only considering the free space path loss and not considering both multipath reflections and co-channel overlaps. We have compared and analyzed the measured and ideal received input voltage.

Finally we have cancelled co-channel overlaps or interferences by guard interval insertions of DVB-T using ATDI ICS Telecom simulation software and recommended ORTO to migrate to DVB-T2 for mitigation of these problems.

Acknowledgement

I would first like to thank my Almighty Allah for everything I have (ALHAMDULILLAH). Secondly I would like thank my thesis advisor Dr. Sultan Feiso of the Electrical Engineering School Head at Addis Ababa Science and Technology University. The door to Dr. Sultan office was always open whenever I ran into a trouble spot or had a question about my research or writing. He consistently allowed this paper to be my own work, but steered me in the right direction whenever he thought I needed it.

Finally, I must express my very profound gratitude to all my family members especially for my mom Sadiya Yasin and my spouse Faiza Mahdi for providing me with unfailing support and continuous encouragement throughout my years of study and through the process of researching and writing this thesis. This accomplishment would not have been possible without them.

Thank you Mother!

Yusuf Jamaal

June 2017

Adama, Ethiopia

Table of Contents

List of Figures

List of Tables

List of Abbreviations

8-VSB	Vestigial Side Band Modulation with 8 discrete amplitude levels
ACI	Adjacent Channel Interference
ATSC	Advanced Television Systems Committee
ATSC-C	ATSC-Cable
ATSC-T	ATSC-Terrestrial
BEM	Block Edge Mask
BER	Bit Error Rate
BMCO	Broadcast Mobile Convergence
BPSK	Binary Phase Shift Keying
CA	Conditional Access
COFDM	Coded Orthogonal Frequency Division Multiplexing
CPU	Central Processing Unit
DQPSK	Differential Quadrature Phase Shift Keying
DSO	Digital Switchover
DTT	Digital Terrestrial Television
DVB	Digital Video Broadcasting
DVB-C	DVB-Cable System
DVB-H	Digital Video Broadcasting – Handheld
DVB-S	DVB-Satellite System
DVB-T	DVB-Terrestrial System
EC	European Commission
EPG	Electronic Program Guide
ETSI	European Telecommunications Standards Institute
EU	European Union
FEC	Forward Error Correction
GE06	Geneva agreement 2006
GPRS	General Packet Radio Service
GPS	Global Positioning System
GSM	Global System for Mobile Communications
GTP	Growth and Transformation Plan
GUI	Graphical User Interface
HDTV	High Definition Television
HTML	Hyper Text Mark-up Language
HTTP	Hyper Text Transport Protocol
IMT	International Mobile Telecommunications
IP	Internet Protocol
IETF	Internet Engineering Task Force
ISDB	Integrated Services Digital Broadcasting
ISDB-C	ISDB-Cable
ISDB-S	ISDB-Satellite
ISDB-T	ISDB-Terrestrial
ISDB-TSB	ISDB-Terrestrial Sound Broadcasting
ISDN	Integrated Services Digital Network
ISP	Interactive Service Provider
ISI	Inter Symbol Interference
ITU-R	International Telecommunication Union for Radio communication

LNA	Low Noise Amplifier
LOS	Line-of-sight
MFN	Multi-Frequency Network
MHP	Multimedia Home Platform
MMDS	Microwave Multipoint Distribution Services
MPEG	Motion Picture Expert Group
OFDM	Orthogonal Frequency Division Multiplexing
ORTO	Oromia Radio and TV Organization
OSD	On Screen Display
OTV	Oromia Television
PAL	Phase Alternating Line
PES	Packetized Elementary Stream
PID	Packet Identification
PSI	Program Specific Information
PSK	Phase Shift Keying
PSTN	Public Switched Telephone Network
PVR	Personal Video Recorder
QAM	Quadrature Amplitude Modulation
QPSK	Quadrature Phase Shift Keying
RF	Radio Frequency
SAS	Subscriber Authorization System
SDTV	Standard Definition Television
SFN	Single-Frequency Network
SI	Service Information
SMS	Subscriber Management System
TC8PSK	Trellis-Coded 8 PSK
TCP	Transmission Control Protocol
UDP	User Datagram Protocol
UHF	Ultra high frequency
VHF	Very High Frequency
UI	User Interface
URL	Universal Resource Locator
VSB	Vestigial Side Band Modulation
WARC	World Administrative Radio Conference
WiMAX	Worldwide Interoperability for Microwave Access
WRC	World Radio communication Conference

1. Introduction

Oromia Radio and TV Organization have launched analog terrestrial TV transmitters in different zonal parts of Oromia in 2008. All these transmitters broadcast analog signal in VHF frequency and MFN. These analog TV signals experience different distortions (ghosting) at receiving end from delayed (echoed) signal caused by different structures, buildings, wind farms and remote transmitter operating at the same frequency (co-channel).

ITU recommends countries in all over the world to migrate from analog broadcasting to digital broadcasting. Oromia Radio and TV Organization is preparing digital switch over strategies to switch off analog transmissions and to launch digital broadcasting.

DVB-T2 is the world's most advanced digital terrestrial television (DTT) system, offering more robustness, flexibility and 50% more efficiency than any other DTT system. It supports SD, HD, UHD, mobile TV, radio, or any combination thereof [1].

DVB-T2 uses OFDM (orthogonal frequency division multiplex) modulation with a large number of subcarriers delivering a robust signal, and offers a range of different modes, making it a very flexible standard [1].

Ghost images (echoes) will be produced during the digital transmission; the pause times called guard intervals will enable these echoes to fade away and do not affect the signal reception.

Guard intervals are used to ensure that different transmissions do not interfere with one another. The number of carriers, guard interval sizes and pilot signals can be adjusted, so that the overheads can be optimized for any target transmission channel.

In COFDM, the beginning of each symbol is preceded by a guard interval. As long as the echoes fall within this interval, they will not affect the receiver's ability to safely decode the actual data, as data is only interpreted outside the guard interval [2].

SFN refers to the broadcasting network with a number of transmitting stations sending the same RF signals at the same frequency in the same time to achieve a reliable coverage in bigger service areas than that of the MFN.

1.1 Problem Statement

OTV is broadcasting PAL standard analog TV signals which are limited in number of television channels offered and reduced quality of audio and video signal.

Due to reflections from mountains, buildings, trees, atmospheres, wind turbines and moving objects, the phase of the OTV RF signal reaching the receiver through different paths will be different, which results in signal fading (Ghosting or delayed image interference) in different locations of OTV coverage area.

OTV Remote transmitters operating at the same frequency in MFN or when two or more television signals on the same frequency appear at the television receiver the input results in co-channel interferences. The effects will happen also when Digital broadcasting in single frequency network (SFN) is launched because all transmitters operate at the same frequency.

These problems could be mitigated by inserting proper guard intervals by synchronization of the main or direct signal to reflected or echoed signal.

1.2 General Objectives

The aim of this thesis is to identify analogue terrestrial OTV reception vulnerability to multi-path reflections and co-channel overlaps, calculating ideal received input voltage and optimizing DVB-T guard intervals to cancel interferences.

Specific Objectives

To measure received input voltage in multipath reflection environment (i.e. Adama).

To measure received input voltage in co-channel overlap (i.e. Bishoftu).

To calculate the ideal received input power at receiver in both multipath reflection and co-channel overlap environments.

To compare the measured input voltage to the required or ideal input voltage at receiver in both multipath reflection and co-channel overlap environments.

To cancel co-channel overlaps or interferences by DVB-T guard interval insertion.

1.3 Scope of Work

The scope of this thesis is to investigate analog OTV signal reflections and overlap effects on sample areas i.e. Adama and Bishoftu cities and their sub-urban. Ideal received input power required to reach receiver will be calculated using friis transmission calculator by only considering free space path loss and not considering multi path reflection and co-channel overlaps. The two results compared and analyzed. Using ATDI ICS Telecom simulation software co-channel overlaps or interferences is decreased by inserting DVB-T guard intervals. Migration to DTT and DVB-T2 guard interval insertions will be recommended to ORTO to optimize OTV SFN signal quality i.e. audio and video at receiving end.

1.4 Thesis Organizations

In chapter 2 we reviewed the literature. In chapter 3 we overviewed DVB – T2 Guard Interval Optimization for SFN. In chapter 4 we have discussed Methodology. In chapter 5 we have discussed our Results and in chapter 6 conclude and gave recommendation.

2. Literature Review

2.1 Introduction

Terrestrial analogue broadcasting was revised by the Regional Radio communication Conference, RRC in Region 1 and changed to digital in considering the advantages in spectrum saving, additional services, different types of services and better quality of service. The first part of this conference, which was held in May 2004 (RRC-04), prepared the planning procedure and parameters; the second part (RRC-06) took place in Geneva in May 2006 and prepared the final frequency plan [4].

Digital techniques offer the possibility not only to trade quality for channel capacity but also to use the available capacity more effectively. Increased demand for channel capacity from commercial broadcasters means that both of these features will need to be exploited. The present situation, with the increasing demand for additional services from commercial operators leads to a demand for more spectrums. This demand can be satisfied by digital systems which offer higher reception quality together with improved spectrum utilization. The launching of digital systems becomes very desirable [4].

In DVB-T multiplexes there is not enough capacity to introduce new services or improve the technical quality of broadcasting contents (SD towards HD and beyond); following the outcome of the last WRC-12 to reduce the amount of spectrum to broadcasting service in favor of mobile services, new and more efficient modulation and transmission techniques will be necessary to satisfy the enhanced TV services (i.e. DVB-T2/HEVC) on DTT platform [4].

2.2 Terrestrial TV Reception Distortions

***Large buildings and structures:* -** Signal reflections are commonplace – buildings or metal structures (like bridges), roads, moving vehicles and even natural features such as hills, cliff faces and trees can reflect signals [3].

Furthermore, if the structure is moving, as in the case of a wind turbine’s rotating blades, the reflections will fluctuate and be quite complex [6].

Analogue television is quite seriously affected by signal reflections, which can give rise to an effect known as "ghosting". Ghosting (or delayed image interference) is where a pale shadow or shadows appear to the right or left of the main picture on television screens [3].

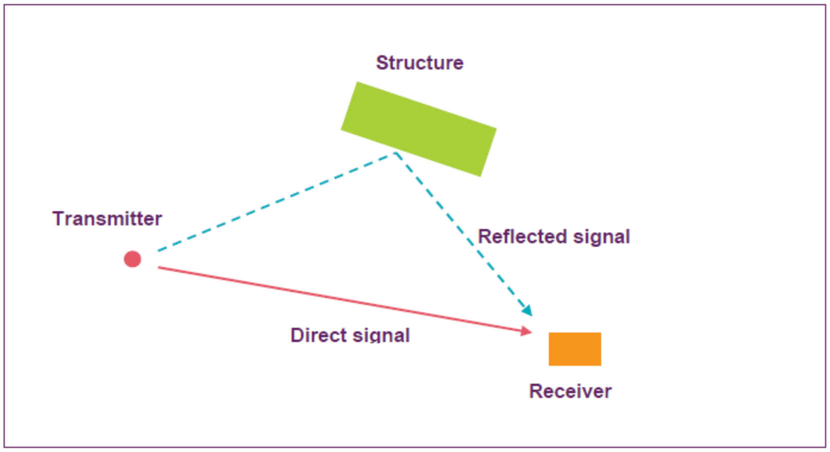

Figure 2.1: Direct and Reflected Signals

Radio transmitter interferences: - A special case of radio transmitter interferences are co-channel interferences when two or more television signals on the same frequency appear at the television receiver input [3].

Co-channel interferences on analogue television produce usually evenly spaced horizontal bars of varying width overlaying the whole picture i.e. the picture is usually still present behind the opaque bars. In severe cases the unwanted television picture will appear in place of the wanted picture [3].

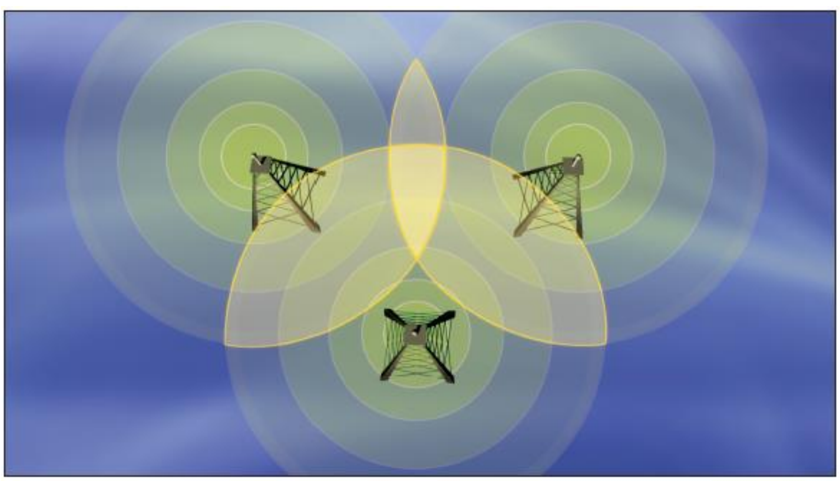

Figure 2.2: Potential co-channel interference

What are Ghosts on Television: TV ghosts are multiple images caused by multiple echoes. In theory, TV signals travel along straight lines. The signal may have a short, direct path between the transmitting antenna and the receiving antenna. The same signal also can reach the receiver antenna over a different, longer echo path because of reflection off nearby buildings and other objects. Under such conditions, the receiver will show two images – a strong, main image and a weaker image, shifted echo or ghost. These ghosts seriously degrade received image quality.

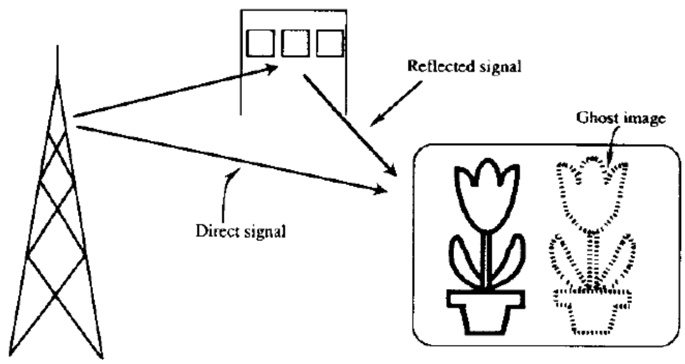

Figure 2.3: Reflection of TV Signal

The Ghosting for conventional television (Analog) cannot be completely eliminated. It can be reduced to a greater extent by signal processing. To carry out signal processing and to make corrections, there is a pre-requisite for a Ghost Cancellation Reference Signal. The specifications for Ghost Cancellation Reference Signals are laid down in ITU-R Recommendations. This signal is used in a GCR Decoder to correct the Ghosting.

2.3 Ghost Cancelling In Analogue Television Systems

Multipath distortion can be mitigated by post processing at the terminal device by transmitting a reference signal [17, 18]. Analogue television broadcast systems can be equipped with a very robust ghost mitigation mechanism where broadcasters need to transmit a reference signal on one of the blanking lines during vertical retrace. This signal is used at the receiver to characterize the channel and to perform adaptive filtering. A world standard ghost cancellation signal was defined in the mid-nineties and now high-end receivers in the consumer market are equipped with circuitry conforming to this standard [18; 19; 20; 21]. This mechanism enables ghosting to be almost completely eliminated. Appelhans and Schroder [22] have researched on ghost cancellation for mobile television, which has greater problems because of the physical motion of the receiver. Many researchers have proposed new ghost cancellation reference signals [23; 24; 25].

2.4 Ghost Cancelling In Digital Television Systems

Many researchers have developed algorithms and techniques to mitigate blocking artefacts. They can be broadly classified into pre-processing [Johnson 1998; Min 1998], post-processing, or some combination of the two [Mancuso 1998] [17].

The simplest post-processing approach is low pass filtering to blur block boundaries. Statistical estimation and set-theoretic reconstruction methods improve on this by making use of the underlying image statistics. Statistical estimation methods use probabilistic models and maximum a priori probabilities to mitigate blocking artefacts. Set-theoretic reconstruction methods uses convex constraint set or the smoothness constraint set to reconstruct the original image by projection on to the convex set. The key idea in POCS is to represent every known property of the original image by a closed convex set. The solution is an image that is an element in all sets and can be found by alternating projections onto each set, starting from the blocky image itself [26; 27; 28; 29] The post-processing algorithms include: the principle of POCS-Projection onto convex sets [20; 30; 31], MRF (Markov random fields) [32], multi-frame constraint sets, maximum-likelihood parameter estimation [25], MAP-maximum a posteriori probability [33; 34], entropy maximization [35], bayesian approaches [36], spatio-temporal concealment using boundary matching algorithm and mesh-based warping [37], multilayer perception for adaptive processing [38] and spatio-temporal adaptive filtering [30]. One drawback of all of these algorithms is their high computational complexity. Any postprocessing should be able to efficiently remove blocking artefacts while preserving dominant edges, retaining the sharpness of the image and not introducing any new artefacts [39].

Carli et al. [40] developed an error concealment technique by data hiding to mitigate blockiness appearing due to loss data packets in transmission. Data hiding techniques can be used to control errors and conceal them by transmitting the redundant information necessary at least to partially recover data lost during transmission.

The wavelet transform embedded data act as a reference signal for both error detection and concealment. Atzori et al. [37] have developed a spatio-temporal concealment technique using boundary matching algorithm and mesh-based warping to conceal errors due to lost data packets in transmission.

Other techniques such as overlap coding, adaptive filtering, application of singularity detection and wavelet transform [41; 31], wavelet-based sub-band decomposition [31], adaptive lapped transform [42], a modified uniform quantisation scheme that constrains local regularity [43], and wavelet transform modulus maxima can be used to mitigate above coding artefacts.

Source coding and channel coding are used in communication to minimise the effects of transmission errors. Source coding techniques are efficient only if the error rate is below an acceptable level (usually in the order of 10^{-6}~10^{-7}). Unequal error protection schemes reduce significantly the occurrence of highly annoying audio and video artefacts [44].

Experimental results of Chang et al. [45] indicate that introducing temporal jitter in video rendering without degrading video quality can be managed with a technique called delay cognizant video coding (DCVC). DCVC segments an incoming video into two video flows with different delay attributes. The DCVC decoder operates in an asynchronous reconstruction mode that attempts to maintain image quality in the presence of network delay jitter [45].

In this thesis we introduce dvb-t2 guard interval optimization for OTV SFN, by the use of OFDM in conjunction with an appropriate choice of guard interval which provides inherently good immunity against the effects of echoes, and that no further ghost cancellation techniques are required.

3. Overview of DVB – T2 Guard Interval Optimization for SFN

3.1 Introduction

DVB-T2 is the 2nd generation standard for digital terrestrial TV, offering significant benefits compared to DVB-T [18].

The emergence of DVB-T2 is motivated by the higher spectral efficiency going along with DVB-T2 – be it for a transition from analogue TV to DVB-T2, be it for a transition from DVB-T to DVB-T2. Higher spectral efficiency means that with the same amount of spectrum, a larger number of programmes can be broadcast or the same number of programmes broadcast with a higher audio/video quality or coverage quality [46].

Alternatively, the coverage area of a digital terrestrial television (DTT) transmitter can be largely increased while keeping constant the transmitter characteristics as well as the reception mode, video quality and number of programmes [46].

DVB-T and DVB-T2; what is the difference?

Compared to DVB-T, DVB-T2 COFDM parameters have been extended to include [46]:

– New generation forward error correction (FEC) (error protection) and higher constellations (256-QAM) resulting in a capacity gain of 25-30%, approaching the Shannon limit.

– OFDM carrier increase from 8k to 32k. In SFN, the guard interval is 1/16 instead of 1/4 resulting in an overhead gain of ~18%.

– New guard interval fractions: 1/128, 19/256, and 19/128.

– Scattered pilot optimization according to the guard interval (GI), continual pilot minimization resulting in an overhead reduction of ~10%.

– Bandwidth extension: e.g. for 8 MHz bandwidth, 7.77 MHz instead of 7.61 MHz (2% gain).

– Extended interleaving including bit, cell, time and frequency interleaving.

The extended range of COFDM parameters allows very significant reductions in overhead to be achieved by DVB-T2 compared with DVB-T, which taken together with the improved error correction coding allows an increase in capacity of up to nearly 50% to be achieved for MFN operation and even higher for SFN operation [18].

DVB-T2 also allows for three new signal bandwidths: 1.7 MHz, 5 MHz and 10 MHz [18].

The DVB-T2 system also provides a number of new features for improved versatility and ruggedness under critical reception conditions such as:

– rotated constellations, which provide a form of modulation diversity, to assist in the reception of higher code-rate signals in demanding transmission channels,

– Special techniques to reduce the peak-to-average power ratio (PAPR) of the transmitted signal resulting in a better efficiency of high power amplifiers multiple transmit antennas,

– Multiple input single output (MISO) transmission mode using a modified form of Alamouti encoding.

At the physical layer, time slicing is included enabling power saving and allowing different physical layer pipes to have different levels of robustness. Sub-slicing within a frame is also possible which increases time diversity/interleaving depth without increasing de-interleaving memory [46].

3.2 System properties

Compared with DVB-T, the DVB-T2 standard offers a bigger choice of the OFDM parameters and modulation schemes. The available bandwidths are also increased. Combining various modulation schemes with Fast Fourier Transform (FFT) sizes and guard intervals allows construction of MFN and SFN networks designed for different applications: from low bit-rate but robust mobile reception to the high bit-rate fixed reception for domestic and professional use [46].

OFDM

The majority of digital terrestrial technologies use multiple carrier orthogonal frequency division multiplexing (OFDM) techniques. Adding forward error correction (FEC) produces coded OFDM (COFDM) to improve the robustness of transmission [47].

OFDM takes a serial data stream to be transmitted and spreads it over a large number of carriers, typically more than a thousand and sometimes many thousands. The data rate conveyed by each carrier is correspondingly reduced and the symbol length is in turn extended. These modulation symbols on each of the carriers are arranged to occur simultaneously. In addition to the data carriers, there are other carriers called pilot carriers or tones which carry information about the radio channel which can be used by a receiver to aid reception [47].

The carrier spacing is uniform and deliberately chosen so that it is the inverse of each symbol duration. This choice of carrier spacing ensures orthogonality of the carriers which means that the influence of adjacent carriers (in fact all other carriers) on the demodulation of a particular carrier is zero. It ensures there is no crosstalk between carriers, even though there is no explicit filtering and their spectra overlap [47]. Figure 3.1 illustrates this.

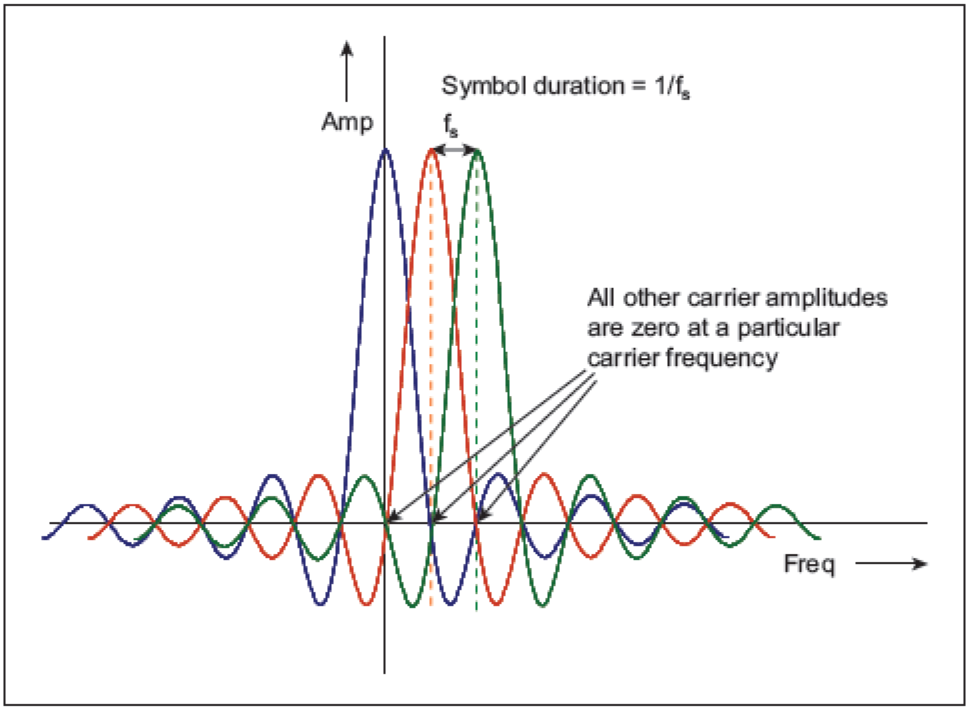

Figure 3.1 Orthogonality

Bandwidth

There are three additional bandwidths available as compared to DVB-T [46].

DVB-T	DVB-T2
–	1.7 MHz
–	5 MHz
6 MHz	6 MHz
7 MHz	7 MHz
8 MHz	8 MHz
–	10 MHz

Table 3.1: Channel bandwidths for DVB-T and DVB-T2

FFT size

While for DVB-T two FFT sizes, 2k and 8k, are specified, DVB-T2 comprises 1k, 2k, 4k, 8k, 16k and 32k FFT sizes [46].

Parameter		1k mode	2k mode	4k mode	8k mode	16k mode	32k mode
Number of carriers, K_{total}	normal carrier mode	853	1705	3409	6817	13633	27265
	extended carrier mode	*n/a*	*n/a*	*n/a*	6913	13921	27841
Value of carrier number, K_{min}	normal carrier mode	0	0	0	0	0	0
	extended carrier mode	*n/a*	*n/a*	*n/a*	0	0	0
Value of carrier number, K_{max}	normal carrier mode	852	1704	3408	6816	13632	27264
	extended carrier mode	*n/a*	*n/a*	*n/a*	6912	13920	27840
Number of carriers added on each side in extended carrier mode, K_{ext} (see Note 2)		0	0	0	48	144	288
Duration, T_U		1024T	2048T	4096T	8192T	16384T	32768T
Duration, T_U μs (see Note 3)		112	224	448	896	1792	3584
Carrier spacing $1/T_U$ (Hz) (see Notes 1 and 2)		*8929*	*4464*	*2232*	*1116*	*558*	*279*
Spacing between carriers K_{min} and K_{max} $(K_{total}-1)/T_U$ (see Note 3)	normal carrier mode	*7.61 MHz*	*7.61 MHz*	*7.61 MHz*	*7.61 MHz*	*7.61 MHz*	*7.61 MHz*
	extended carrier mode	*n/a*	*n/a*	*n/a*	*7.71 MHz*	*7.77 MHz*	*7.77 MHz*

NOTE 1 – Numerical values in italics are approximate values.
NOTE 2 – This value is used in the definition of the pilot sequence in both normal and extended carrier mode.
NOTE 3 – Values for 8 MHz channels.

Table 3.2: FFT size parameters for DVB-T2/8 MHz

For 8 MHz bandwidth channels, the spacing of sub-carrier frequencies Δf, which also represents the useful symbol rate R_u, can be written as [21]

$$\Delta f = R_u = B_k / n$$

n = number of orthogonal sub-carrier waves B_k = bandwidth of the assigned frequency channel

n = 2048 (for **2k** mode), n = 8192 (for **8k**mode) and B_k = (for video broadcasting 8, 7, 6 MHz)

The corresponding useful time is symbol T_u is then

$$T_u = (R_u)^{-1}$$

This time is then further extended by the so-called **guard interval** T_G or Δ, which is often defined as a part (k_T) of symbol time, i.e.

$$k_T = T_G/T_u = 1/4, 1/8, 1/16, 1/32.$$

In the guard interval T_G, no useful information is transmitted. It is used to eliminate reception of delayed signals and thus influences the possible choice of transmitter distances in the single frequency network [49].

The total lengths of extended symbols [49]

$$T_s = T_u + T_G$$

The velocity of lights is c=299792448m/s which results in signal delay per kilometer transmitter distance of t_{1km}=3.336 μs.

Modulation scheme

In DVB-T2, the additional 256-QAM modulation scheme is available, see Table 3.3. The new error protection techniques allow the usage of such high modulation schemes [46].

DVB-T	DVB-T2
QPSK	QPSK
16-QAM	16-QAM
64-QAM	64-QAM
–	256-QAM

Table 3.3: Modulation schemes for DVB-T and DVB-T2

Inter-symbol interference

In order to demodulate the signal – and looking at only one carrier – the receiver has to evaluate the symbol during the symbol duration. Three consecutive symbols in time, denoted by n-1, n and n+1, and the setting of the FFT-window such that symbol n is evaluated by the receiver, are shown in Figure 3.2. No guard interval is used in this example, and the FFT-window has the same duration as the symbol [48].

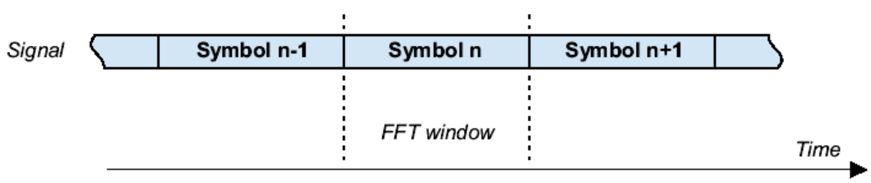

Figure 3.2: OFDM symbol duration and FFT-window (no guard interval)

In an environment where several useful signals—either from multipath echoes or from other transmitters in an SFN—are available to the receiver, things become more complex. Usually, the signals arrive at different times at the receiver which, in the absence of a guard interval, makes correct synchronization to all of the signals impossible. Such a situation with two signals as an example is depicted in Figure 3.3. Synchronization to symbol n of signal 1 leads to an overlap of the FFT-window with the preceding symbol n–1 of the delayed signal 2. Since this symbol n–1 carries different information from symbol n, the overlap acts as interference to the evaluation of symbol n. The degradation of the reception caused by this mechanism is called inter-symbol interference (ISI) [48].

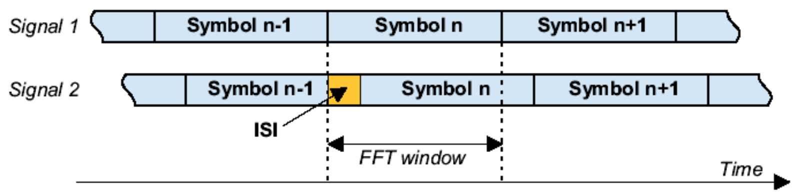

Figure 3.3: Inter-symbol interference with a delayed signal (no guard interval)

Guard Interval

In order to overcome the inter-symbol interference problem in DVB-T, DVB-T2 and T-DAB, part of the symbol is copied from the beginning of the symbol to the end, increasing its duration by a certain amount of time called the guard interval. This cyclic prolongation of the original symbol is shown in Figure 3.4. The guard interval is denoted by Δ [48].

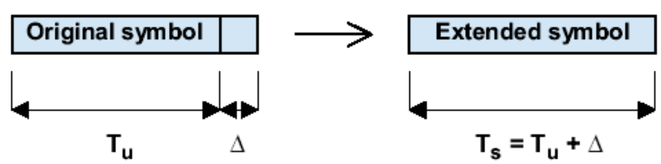

Figure 3.4: Increase of the symbol duration by the guard interval

The new increased symbol duration is denoted by Ts and the original symbol duration is often called useful symbol duration Tu. The duration of the FFT-window during which the symbol is evaluated is kept at the original value Tu. The orthogonal relationship is kept with the original symbol duration T_u, not the extended T_s [48].

The improvement that is achieved by the insertion of the guard interval can be seen from Figure 3.5 with two signals as an example. The guard interval now allows for the FFT-window to be positioned so that there is no overlap with a preceding or subsequent symbol, thus avoiding ISI [48].

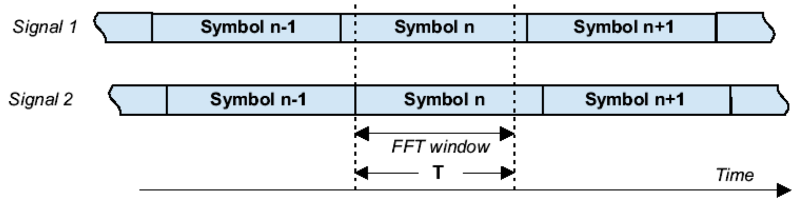

Figure 3.5: Guard interval utilization

The insertion of the guard interval reduces the data capacity because not all of the symbol duration T_s is used for "useful" data [48].
In a multipath or SFN environment, where many potentially useful signals are available to the receiver, the choice of the FFT-window position becomes more complex. A number of different strategies that can be applied are discussed in the next chapter [48].

All signals with time delays that cannot be absorbed by the guard interval in the way described above introduce a degradation of reception, similar to that shown in Figure 3.3. Any part of each of these received signals that falls outside the guard interval has an interfering characteristic [48].
A further refinement adds the concept of a guard interval. Each symbol is transmitted for a duration which is longer than the active symbol portion by a period called the guard interval. It is generated by copying the last fraction of the active symbol and placing it at the front of the active symbol period as shown in figure 3.6 [47].

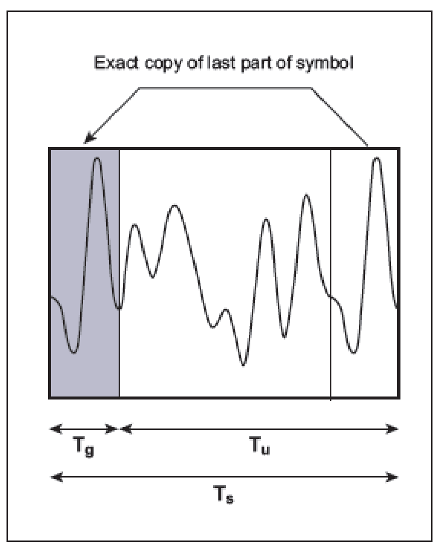

Figure 3.6: Guard Interval generation

The consequence is that a receiver will not experience either inter-symbol or inter-carrier interference provided that any secondary direct signals from co-channel transmitters or multi-path echoes present have a delay which does not exceed the guard interval [47].

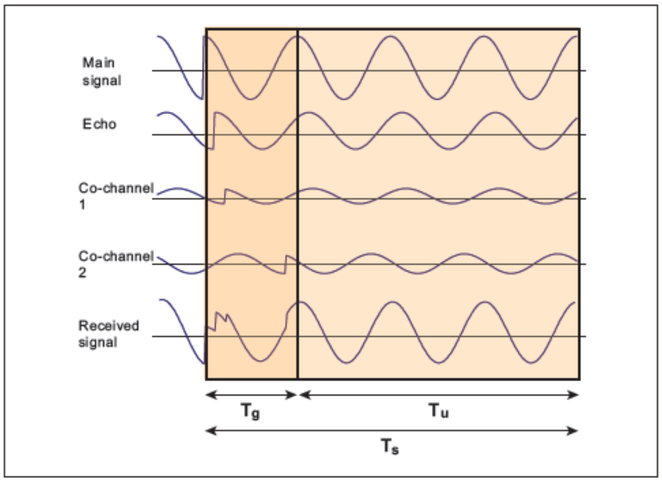

Figure 3.7: All signals received within Guard Interval

Figure 3.7 shows the reception of the main signal and its echo plus two co-channel signals from other transmitters. All signals are received within the guard interval, after which steady state of the channel is attained and evaluation of the symbol can commence [47].

OFDM, due to its multicarrier nature, exhibits relatively long symbols. This long symbol period already provides a certain degree of protection against inter-symbol interference caused by multipath propagation. However, as described above, this protection is greatly enhanced by use of the guard interval. The guard intervals for the 2k and 8k DVB-T systems are given in Table 3.4 below [48].

Mode	**8k mode**				**2k mode**			
	Guard Interval							
	1/4	1/8	1/16	1/32	1/4	1/8	1/16	1/32
8 MHz channel	224 µs	112 µs	56 µs	28 µs	56 µs	28 µs	14 µs	7 µs
7 MHz channel	256 µs	128 µs	64 µs	32 µs	64 µs	32 µs	16 µs	8 µs
6 MHz channel	*298.667 µs*	*149.333 µs*	*74.667 µs*	*37.333 µs*	*74.667 µs*	*37.333 µs*	*18.667 µs*	*9.333 µs*

NOTE – values in italics are approximate values.

Table 3.4: The guard intervals for the 2k and 8k DVB-T systems

As the proportion of the symbol used to make the guard interval is increased, the transmission capacity decreases [48].

The following Table 3.5 gives the absolute guard interval duration Δ, expressed in multiples of the elementary period T2 for each combination of FFT size and guard interval fraction for DVB-T2 system [48].

FFT size	Guard interval fraction (Δ/T_u)						
	1/128	1/32	1/16	19/256	1/8	19/128	1/4
32K	256T	1 024T	2 048T	2 432T	4 096T	4 864T	NA
16K	128T	512T	1 024T	1 216T	2 048T	2 432T	4 096T
8K	64T	256T	512T	608T	1 024T	1 216T	2 048T
4K	NA	128T	256T	NA	512T	NA	1 024T
2K	NA	64T	128T	NA	256T	NA	512T
1K	NA	NA	64T	NA	128T	NA	256T
NOTE – There are further restrictions on the combinations of FFT size and guard interval allowed for T2-Lite							

		GI-Fraction						
		1/128	**1/32**	**1/16**	**19/256**	**1/8**	**19/128**	**1/4**
FFT	**T_U(ms)**	**GI (µs)**						
32k	3.584	28	112	224	266	448	532	*n/a*
16k	1.792	14	56	112	133	224	266	448
8k	0.896	7	28	56	66.5	112	133	224
4k	0.448	*n/a*	14	28	*n/a*	56	*n/a*	112
2k	0.224	*n/a*	7	14	*n/a*	28	*n/a*	56
1k	0.112	*n/a*	*n/a*	7	*n/a*	14	*n/a*	28

Table 3.5: The guard intervals for the DVB-T2 systems

Table 3.6 gives the absolute values of *T* for all the available bandwidths. With these the parameter values for the other bandwidths can be calculated [46].

Bandwidth	1.7 MHz	5 MHz	6 MHz	7 MHz	8 MHz	10 MHz (see Note)
Elementary period, *T*	71/131 µs	7/40 µs	7/48 µs	1/8 µs	7/64 µs	7/80 µs

Table 3.6: Elementary period as a function of bandwidth

Available data rate

Tables 3.4, 3.5 and 3.6 show the large number of possible modes in DVB-T2. Some of the 2k and 8k modes are the same as in DVB-T. The main difference is the addition of 16k and 32k FFT [46].

Modulation	Code rate	Absolute maximum bit-rate			Recommended configuration		
		Bit rate Mbit/s	Frame length, L_F	FEC blocks per frame	Bit rate Mbit/s	Frame length, L_F	FEC blocks per frame
QPSK	1/2	7.49255	62	52	7.4442731	60	50
	3/5	9.003747			8.9457325		
	2/3	10.01867			9.9541201		
	3/4	11.27054			11.197922		
	4/5	12.02614			11.948651		
	5/6	12.53733			12.456553		
16-QAM	1/2	15.03743	60	101	15.037432	60	101
	3/5	18.07038			18.07038		
	2/3	20.10732			20.107323		
	3/4	22.6198			22.619802		
	4/5	24.13628			24.136276		
	5/6	25.16224			25.162236		
64-QAM	1/2	22.51994	46	116	22.481705	60	151
	3/5	27.06206			27.016112		
	2/3	30.11257			30.061443		
	3/4	33.87524			33.817724		
	4/5	36.1463			36.084927		
	5/6	37.68277			37.618789		
256-QAM	1/2	30.08728	68	229	30.074863	60	202
	3/5	36.15568			36.140759		
	2/3	40.23124			40.214645		
	3/4	45.25828			45.239604		
	4/5	48.29248			48.272552		
	5/6	50.34524			50.324472		

Table 3.7: Maximum bit-rate and recommended configurations for 8 MHz, 32k 1/128, PP7

The very long symbol time will, in principle, result in a poorer Doppler performance, due to the short inter-carrier distance in the OFDM signal. The 32k mode is therefore aimed mainly at fixed rooftop reception. Laboratory and field tests indicate that the 32k mode is unlikely to be used to provide mobile (vehicular) reception at UHF. Even in a portable (indoor or outdoor pedestrian) receiving environment with relatively low Doppler frequencies it needs to be confirmed that the 32k mode is suitable. The Doppler performance is however up to 4 times better at VHF compared to UHF Band V. This fact may make VHF Band III frequencies interesting for providing mobile services using the DVB-T2 system [46].

One additional difference between DVB-T and DVB-T2 is the increased number of GI fraction using 1/128, 19/256 and 19/128, which gives further possibilities to adopt the length of the guard interval to the size of the SFN [46].

3.3 Principle of the SFN

The signal coverage of a certain area can be provided by a number of transmitters, transmitting the multiplex of digital television or radio signals in the identical frequency channel. Their partial signal contributions in the reception point not only do not interfere, under certain circumstances then even improve the reception. It is thus obvious that single frequency networks of digital transmitters may considerably improve the utilization of frequency bands and channels as well as energy balance of digital transmitters.

Digital transmitters in SFN might be considerably lesser power for the signal coverage of the given area sufficient for quality reception. Methods of SFN cannot be used with the terrestrial analogue television broadcasting, where in fact all the present-day world's television standards use amplitude vestigial sideband modulation and operate in multi-frequency networks MFN (Multi Frequency Network) [49].

In SFN, all transmitters are modulated with the same signal and radiate same frequency. The limiting effect of SFN technique is self-interference of the network. If signals from far distant transmitters are delayed more than allowed by the guard interval they behave as noise-like interfering signals rather than wanted signals. The self-interference of SFN for a given transmitter spacing is reduced by selecting a large guard interval. The network generated self-interference of an SFN can be kept sufficiently low by a careful choice of the system parameters and transmitter powers [50].

There are two main methods of creating a single- frequency network. The first is through the use of on channel boosters. On-channel boosters quickly receive the OTA signal from the main tower and retransmit the signal at the same frequency. The problem is that there is no error correction. So, any errors in receptions are simply retransmitted along with the slight echo caused by the booster itself. With distributed transmission, the signal is delivered to each of its transmitters via fixed channels (land-based delivery). Then through the use GPS based reference clocks at each tower (for both time and frequency), the signals are synced so each can emit a perfect copy of both the signal and the symbol data. To get each transmitter synchronized in both the time and frequency domains some extra data is added to the serial data streams (these contain the encoded audio and data inputs) sent to the transmitters. This additional data stream is essentially a time reference signal inserted into the network. At each transmitter the OFDM modulator uses this time stamp to calculate the local delay so that a common on-air time is achieved [50].

The effects of multipath occur within SFNs. This is because waves from different towers have potential to reach an antenna at different times and a receiver's ability to handle multipath is paramount to its success. With the SFN technique, large areas can be served with common multiplex at a common radio center frequency. The frequency efficiency of SFNs appears to be very high compared to MFNs. The SFN technique is also power efficient [50].

The advantage of the SFN approach is:

- High frequency efficiency
- Low-power operation (internal network gain)
- High location probability
- Easy gap-filling (frequency re-use)

The disadvantages are:

- Network splitting is not possible
- Synchronization is necessary
- Feed control is required [22]

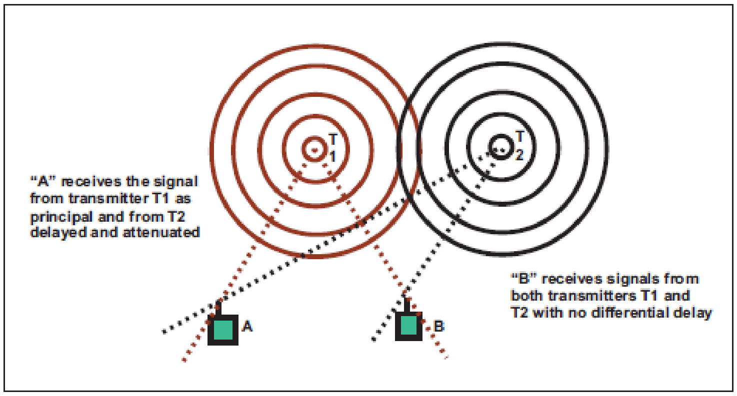

Figure 3.8: Single Frequency Network configuration

Figure 3.8 shows a basic SFN configuration. Assuming there are no programmed delays through the transmitters themselves so that each transmits the same symbol at the same time, then receiver "A" does not suffer any inter-symbol interference if the delay difference between the signals from transmitters T1and T2 is less than the guard interval. The phase difference of the two signals received at "A" will likely cause some fading effects across the channel which can be compensated by the information supplied with the pilot carriers. At receiver "B", the propagation time from both transmitters is identical and no differential delay effects will occur [47].

3.4 Choice of System Parameters to Optimize DVB-T2 Guard Intervals

Guard Interval Impact on Bitrate

Having a large guard interval obviously has an impact on the efficiency of the bitrate and also on the number of carriers.

The bit rate can be calculated using the following equation:

$$\textit{Useful Data Bit Rate} = \frac{B*C*M*N}{T} \text{ bits per second}$$

Where:

B = Efficiency of Reed Solomon bloc code

C = Convolution code rate

M = Number of bits per carrier

N = Number of data carrier used

T = Total Duration of the symbol including the guard interval

Choice of FFT size

The results of choosing a certain FFT size are well known: an increased FFT size will give a greater delay tolerance for the same fractional guard interval, allowing larger SFNs to be constructed. Alternatively, a larger FFT size allows the same delay tolerance to be achieved with a smaller overhead due to the guard interval [46].

A larger FFT size implies a longer symbol duration, which means that the guard interval fraction is smaller for a given guard interval duration in time (see, for example, Fig. 3.9). This reduction in overhead leads to an increase in throughput ranging from 2.3% to 17.6% [46].

Figure 3.9: Guard interval overhead reduction with larger FFT size

For mobile reception in UHF Band IV/V, or higher bands, smaller FFT sizes should be used as they offer better Doppler performance. The 1k FFT mode which offers the highest Doppler performance is intended primarily for operation in the L-band (about 1.5 GHz), or higher, using a nominal occupied bandwidth of 1.7 MHz [46].

For delivering high-bit-rate services to fixed rooftop antennas, in VHF or UHF, the 32k FFT mode is more appropriate. In this situation the time variations in the channel are minimized, and 32k offers the very highest bit rates achievable using DVB-T2 [46].

For a given FFT size, constellation and code rate, the Doppler performance is roughly proportional to the RF bandwidth (halving the bandwidth will halve the carrier spacing resulting in half the Doppler performance) and inversely proportional to the RF frequency and therefore higher frequencies are more vulnerable to fast time-varying channels, having poorer Doppler performance [46].

On the other hand, increasing the FFT size would proportionally decrease the Doppler performance of the system.

Selection of DVB-T2 Mode for SFNs

One approach for selecting a mode for SFN operation would be to select the length of the guard interval according to the physical size of the SFN or the SFN’s intra transmitter separation distances, noting of course that it may be possible to have larger transmitter separations than the guard interval depending on practical considerations such as terrain, propagation and system robustness, etc. Additionally, optimization of coverage by modification of antenna diagrams, transmitter powers, antenna heights, transmitter timing, etc. may allow larger transmitter distances in the SFN than the guard interval [46].

The GI fraction involves consideration of the FFT size which is related to the reception scenario: fixed rooftop, portable or mobile reception.

In the case of fixed rooftop reception it would seem desirable to use 32k or 16k FFT as a larger FFT size would reduce the GI fraction and increase the available capacity.

For portable and mobile reception a lower FFT size such as 16k, 8k or even 4k may need to be considered, in particular for mobile reception when Doppler is a limitation [46].

The choice of modulation determines the bit rate (capacity), but it also has a large impact upon the robustness of the system; higher order modulation schemes that offer more capacity are more fragile. DVB-T2, compared with DVB-T, 256-QAM will require C/N values in the same order of magnitude as those previously required for 64-QAM, that is, values in the order of 17-20 dB [46].

Increased system robustness will also have a large impact upon SFN performance since a lower required C/N will reduce the susceptibility for SFN self-interference.

4. Methodology

4.1 Introduction

The thesis methodology in this topic helps as a model to achieve the objective of this study. This methodology is carried out according to the model or flow chart shown (see Figure 3.1) below. First step is to find mathematical model of multipath distortions at receiving end i.e. for echoes and overlaps of TV signals. The system specification i.e. Tx and Rx configuration, Channel modeling and guard interval insertion techniques will be determined. Calculating the multipath distortions (signal delay) and multiple or different field strength values at a receiving point will be presented and guard interval is a method to cancel multipath distortions by comparing the resulting values will be shown. A scenario or a measurement will be made for urban, sub-urban and rural areas.

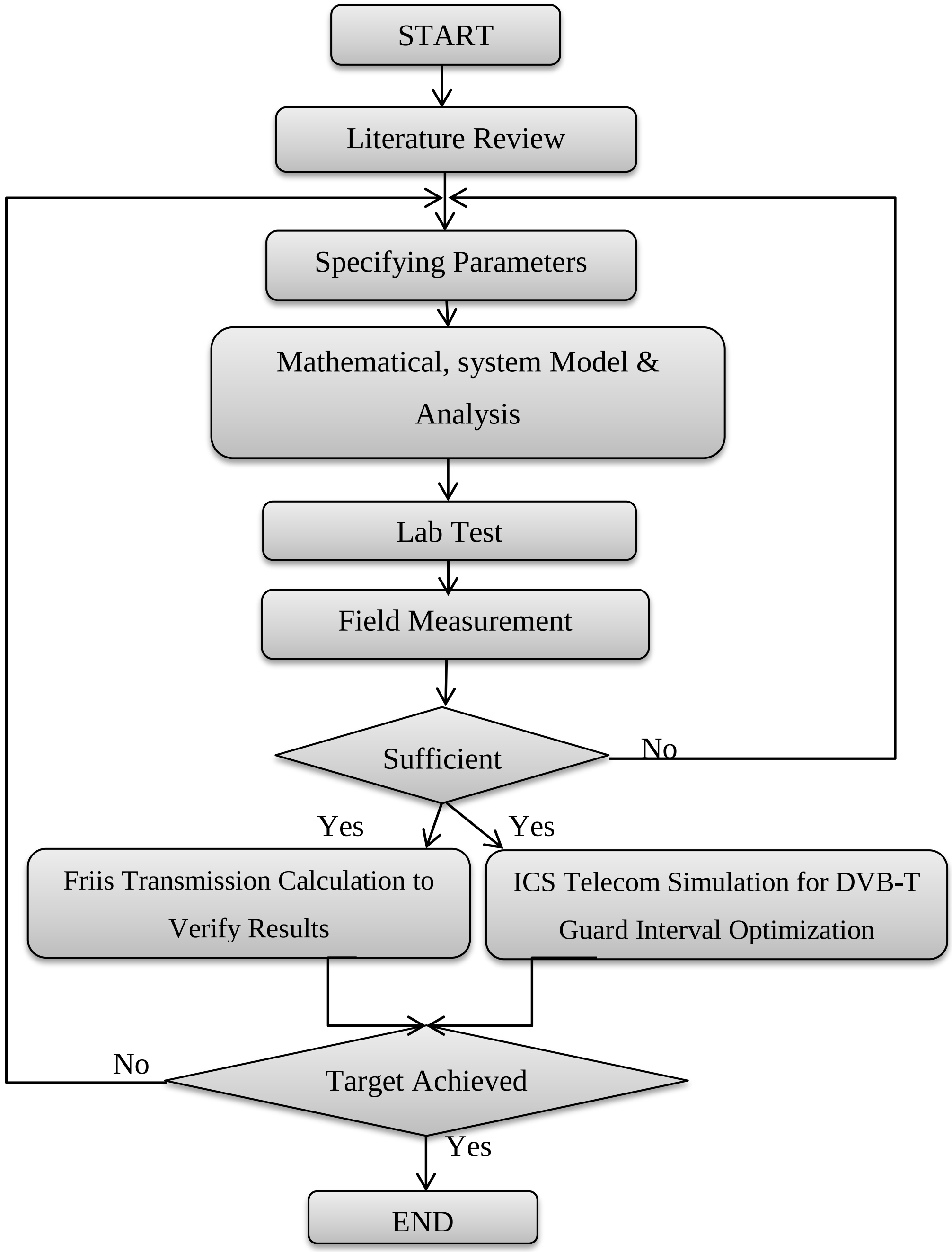

Figure 4.1: Thesis Methodology Flow Chart

4.2 Data Collection

Data collection will be done based on the articles studied i.e. field measurement of OTV signal at receiver. Collected data consists of all information which is needed to be collected such as OTV signals received input voltage which are affected by multipath reflections and co-channel overlaps and system parameters.

4.3 Mathematical Model

Minimum Signal Level: In order to determine minimum receiver field strength, the SNR must be specified which its value on the output image of an ordinary TV set is approximately a minimum of 30-33dB, and for vestigial side band (VSB) receivers, it is about 38-41dB.
The specified point may be expressed by

$$SNR = S/N = 20\log(V_r/V_n) \quad \ldots 4.1$$

Where V_r is a receiver input voltage level and V_n is the equivalent voltage level of noise temperature at the receiver input which has a relation in the logarithmic scale:

$$V_n\,(dB_{\mu v}) = 10\log(kT_0BR) + F + 120 \quad \ldots 4.2$$

Where;
K: Boltzmann constant equal to $1.38\text{x}10^{-23}$
T_0: Reference temperature equal to 290^0K
B: Bandwidth of the receive in Hz
R: Input impedance of the receiver in ohms
F: Receiver noise figure
The (3.2) can be rewritten in the following form:

$$V_r\,(dB_{\mu v}) = (SNR)_{min} + V_n\,(dB_{\mu v}) \quad \ldots 4.3$$

Also, the relation of electrical field strength with the input voltage of the receiver using an isotropic antenna is given by

$$E_r = V_r + L - G - 33.6 + 20\log f \quad \ldots 4.4$$

For dipole antenna the equation is

$$E_r = V_r + L - G_d - 32 + 20\log f \quad \ldots 4.5$$

Where;

E_r: Received electrical field strength in $dB_{\mu v/m}$

V_r: Voltage at the input port of receiver in $dB_{\mu v}$

L: Feeder Loss in dB

G: Antenna gain of receiver relative to isotropic antenna in dB_i

G_d: Antenna gain of relative to dipole antenna in dB_d

f : Radio channel frequency in MHz

Friis Equation: is used to find the ideal power received at an antenna from basic information about the transmission.

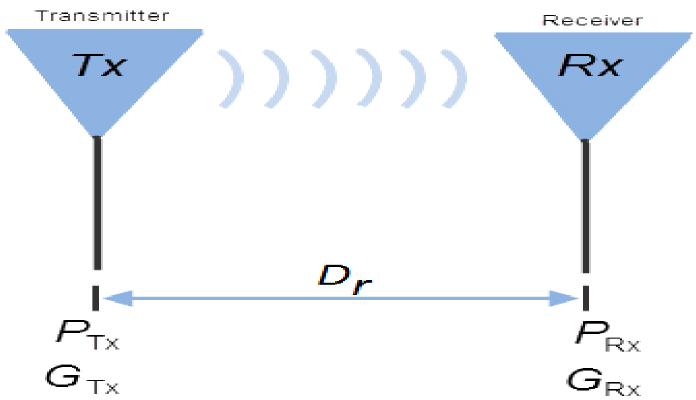

Figure 4.2: Friis Transmission

Pasternack's Friis Transmission Equation calculates the received power from an antenna at some distance given a transmission frequency and antenna gains.

$$P_{rx} = P_{tx}G_{tx}G_{rx}\left(C/4\pi D_r f_0\right)^2 \ldots\ldots\ldots\ldots\ldots\ldots\ldots\ldots\ldots\ldots\ldots\ldots\ldots\ldots\ldots 4.6$$

$$P_{rx}(dB) = P_{tx} + G_{tx} + G_{rx} + 20\log_{10}\left(\lambda / 4\pi D_r\right) \ldots\ldots\ldots\ldots\ldots\ldots\ldots\ldots\ldots 4.7$$

P_{rx}: Received power in W/mW

P_{tx}: Transmitted power in W/mW

G_{tx}: Transmitter Antenna gain in dB

G_{rx}: Receiver Antenna gain in dB

C: Speed of light in m/s

f_0: Channel frequency in MHz

D_r: Separation distance between tnasmitter and receiver in m/km

λ: Wave length in m

Z: Input impedance

For equation (3.6) power is in W/mW for equation (3.7) the power is in dBm/dBW.

Watts to dBm Conversion

$$P\ (dBm) = 10 \log_{10} \left(P\ (w)\right) \ldots\ldots\ldots 4.8$$

dBm to dBµV Conversion

$$dB\mu v = 90 + 10\log(Z) + dBm \ldots\ldots\ldots 4.9$$

Free Space Path Loss Equation: calculates the loss (in dB) between two antennas where the gain, distance and frequency are known.

$$FSPL = 20 \log_{10}(d) + 20 \log_{10}(f) + 20 \log_{10}(4\pi/c) - G_t - G_r \ldots\ldots\ldots 4.10$$

Free Space Path Loss (FSPL) calculations are often used to help predict RF signal strength in an antenna system. Loss increases with distance.

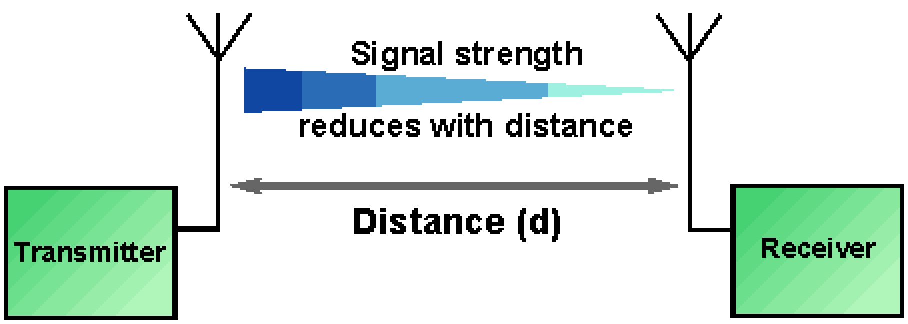

Figure 4.3: Free Space Path Loss

4.4 Analysis

Multipath Propagation: Multipath occurs when a signal takes two or more paths from the transmitting antenna to the receiving antenna.

We'll assume that one signal, the *direct ray*, travels directly from the transmitter to the receiver. The other signals (or *rays*) arrive at the receiving antenna via more roundabout paths. In our analysis, we'll assume these indirect rays arrive after the direct ray and that the indirect rays are weaker in power than the direct rays.

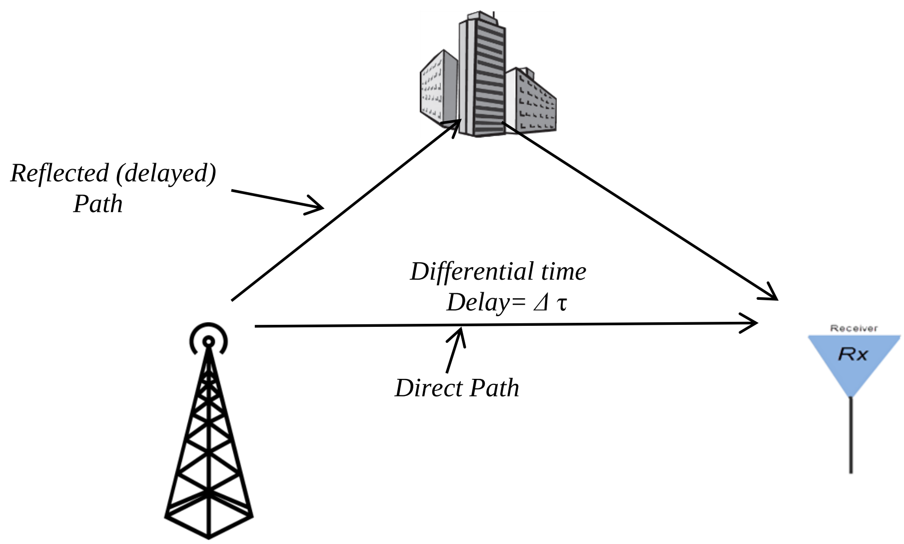

Figure 4.4: Multipath Propagation

The equation for the direct signal is

$$V_D\,(t) = \cos\,(\omega_0 t) \quad \text{......4.11}$$

Where

$\omega_0 = 2\pi\, f_0$ = the angular operating frequency

We'll assume the amplitude of the direct ray is unity and the phase angle is zero. The equations for the reflected rays are

$$\begin{aligned} V_{R,\,1} &= A_1 \cos\,[\omega_0\,(t - \tau_1)] \\ V_{R,\,2} &= A_2 \cos\,[\omega_0\,(t - \tau_2)] \\ &\;\;. \qquad\qquad\qquad\qquad \text{......4.12} \\ &\;\;. \\ &\;\;. \\ V_{R,\,n} &= A_n \cos\,[\omega_0\,(t - \tau_n)] \end{aligned}$$

Where

A_n = a real number describing the difference in amplitude between the direct ray and the *n*-th reflected ray

τ_n = the time difference of arrival between the direct and the *n*-th reflected ray. The *n*-th ray arrives τ_n seconds after the direct ray.

We may find it convenient to rewrite the equations of (4.12) as

$$V_{R,1} = A_1 \cos(\omega_0 t + \phi_1)$$
$$V_{R,2} = A_2 \cos(\omega_0 t + \phi_2)$$
$$\vdots \qquad \qquad \text{(4.13)}$$
$$V_{R,n} = A_n \cos(\omega_0 t + \phi_n)$$

Where

$\phi_1 = -\omega_0 \tau_1$

$\phi_2 = -\omega_0 \tau_2$

$\phi_n = -\omega_0 \tau_n$

For our analysis, we assume that the direct and reflected waves have different amplitudes (described by A_n) and that the waves arrive at the receiving antenna at slightly different times (described by τ_n).

The characteristics of multipath channels usually change over time because the geometry of the channel changes.

Two-Ray Analysis: The two-ray multipath analysis assumes that only two rays are present at the receive antenna: the direct ray V_D (t) and a single reflected ray $V_{R,1}$(t). The two signals present at the receive antenna are

$$V_{Rx}(t) = V_D(t) + V_{R,1}(t) \qquad \text{..............................4.14}$$

$$= \cos(\omega_0 t) + A_1 \cos(\omega_0 t + \phi_1)$$

Where

$$\phi_1 = -\omega_0 \tau_1$$

We'll experience a multipath fading event when the received signal power falls below some arbitrary threshold. Analysis of equation (4.14) reveals

$$V_{Rx}(t) = 0 \text{ whenever } \begin{cases} A_1 = 1 \\ \phi_1 = 180^0 \end{cases} \qquad \text{.................................4.15}$$

Calculation between phase angle ϕ^0 in degrees (deg), the time delay $\Delta\tau$ and the frequency f is:

$$\phi^0 = 360^0 * f_0 * \Delta\tau \text{ ....4.16}$$

As Figure 4.5 shows, we can interpret equation (4.14) as the addition of two phasors. The direct ray is represented by a phasor of unity length at 0^0, whereas the indirect ray is represented by a phasor of length A_1 at an angle of ϕ_1. Figure 4.5 also shows the locus of the resultant vector as the phase of the indirect ray varies over 0^0 to 360^0.

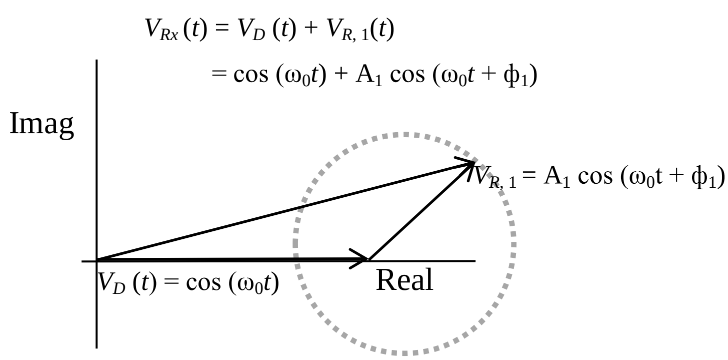

Figure 4.5: The geometric phasor interpretation of equation (4.14)

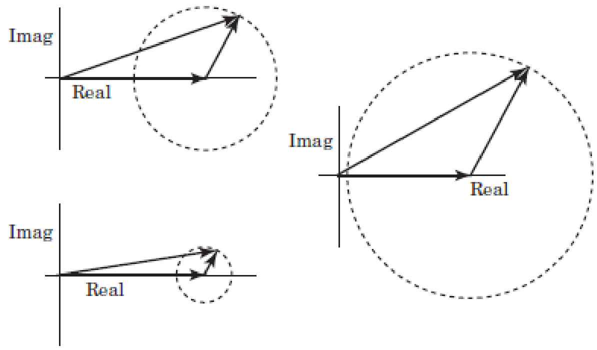

Figure 4.6: The phasor interpretation of equation (4.14) for various values of A_1.

Figure 4.6 shows the phasor diagrams for several values of A_1. The resultant vector $V_{Rx(t)}$ almost equals the direct ray when A_1 is very small. As a result, the receiver sees a nearly undistorted signal. As A_1 approaches unity, the phase and amplitude of $V_{Rx(t)}$ change wildly with the phase of the indirect ray.

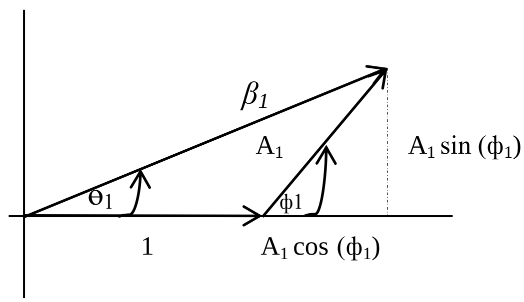

Figure 4.7: Phasor analysis of two-ray multipath.

$$(\beta_1)^2 = \left[1 + A_1 \cos(\phi_1)\right]^2 + \left[A_1 \sin(\phi_1)\right]^2$$

$$= 1 + 2\,A_1 \cos(\phi_1) + A_1^2 \cos^2(\phi_1) + A_1^2 \sin^2(\phi_1)$$

$$= 1 + 2A_1 \cos(\phi_1) + A_1^2$$

$$\tan(\theta_1) = \frac{A_1 \sin(\phi_1)}{1 + A_1 \cos(\phi_1)}$$

Vector analysis of Figure 4.7 allows us to rewrite equation (4.14) as a single cosine with amplitude and phase change

$$V_{Rx}(t) = \cos(\omega_0 t) + A_1 \cos(\omega_0 t + \phi_1) \text{ ....…..4.17}$$

$$= \beta_1 \cos(\omega_0 t + \theta_1)$$

Where

$$(\beta_1)^2 = 1 + 2A_1 \cos(\phi_1) + A_1^2$$

$$\theta_1 = \tan^{-1}\left(\frac{A_1 \sin(\phi_1)}{1 + A_1 \cos(\phi_1)}\right) \quad \text{………………………………………4.18}$$

The worst signal attenuation occurs when A_1 is unity and ϕ1 is 180^0. The received signal is completely canceled under these conditions.

Increase in received signal strength is whenever

$$-90^0 \leq \phi_1 \leq 90^0 \text{ ……………………………………………………4.20}$$

The maximum increase is when A_1 is unity and ϕ_1 is 0^0. The received signal is the sum of the direct and reflected ray and increase in amplitude.

The same A_1 produces the maximum increase in signal power also produces the worst attenuation based on the phase ϕ_1. Multipath affects the phase of the received signal as well as its amplitude.

Three-Ray Analysis: we can extend our two-ray analysis of multipath into a three-ray model. The direct ray is given by

$$V_D(t) = \cos(\omega_0 t)$$

The two reflected rays are

$$V_{R,1} = A_1 \cos[\omega_0 (t - \tau_1)]$$

$$V_{R,2} = A_2 \cos[\omega_0 (t - \tau_2)]$$

Received signal by an antenna

$$V_{Rx}(t) = \cos(\omega_0 t) + A_1 \cos[\omega_0 (t - \tau_1)] + A_2 \cos[\omega_0 (t - \tau_2)] \quad \ldots\ldots\ldots\ldots\ldots 4.21$$

$$= \cos(\omega_0 t) + A_1 \cos(\omega_0 t + \phi_1) + A_2 \cos(\omega_0 t + \phi_1)$$

Where

$\phi_1 = -\omega_0 \tau_1$

$\phi_2 = -\omega_0 \tau_2$

As in the two-ray analysis, we can rewrite equation (3.21) as

$$V_{Rx}(t) = \beta_2 \cos(\omega_0 t + \theta_2) \quad \ldots\ldots\ldots\ldots\ldots\ldots\ldots\ldots\ldots\ldots\ldots\ldots 4.22$$

Where

$$(\beta_2)^2 = 1 + A_1^2 + A_2^2 + 2A_1 \cos(\phi_1) + 2A_2 \cos(\phi_2) \quad \ldots\ldots\ldots\ldots\ldots 4.23$$

$$+ 2A_1 A_2 \left\{ \cos(\phi_1)\cos(\phi_2) + \sin(\phi_1)\sin(\phi_2) \right\}$$

$$\theta_2 = \tan^{-1}\left(\frac{A_1 \sin(\phi_1) + A_2 \sin(\phi_2)}{1 + A_1 \cos(\phi_1) + A_2 \cos(\phi_2)} \right) \quad \ldots\ldots\ldots\ldots\ldots\ldots 4.24$$

***n*-Ray Analysis**: We can easily extend the three-ray multipath model to an *n*-ray model. We assume that *n* separate signals arrive at the receiving antenna, each with its own A and τ.

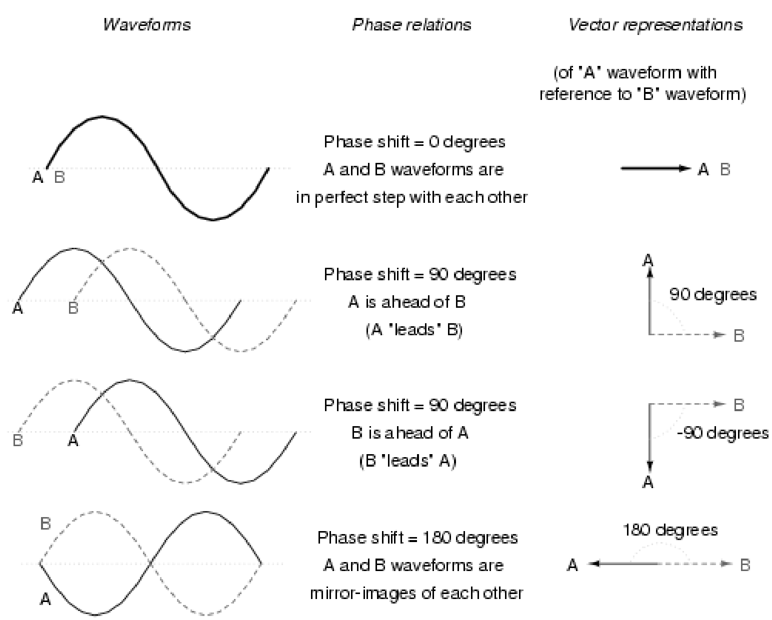

Figure 4.8: Phase Relation of waves

4.5 System Model

We have put our system model for performing multipath reflection (echoes) effects and co-channel interference (channel overlaps or remote transmitter interference) by measurements, tests and simulation.

Lab Test Model

We have used Agilent N9320A spectrum analyzer to generate 10MHz reference clean RF and connected to DS1191 analyzer to view the clean spectrum and received input voltage.

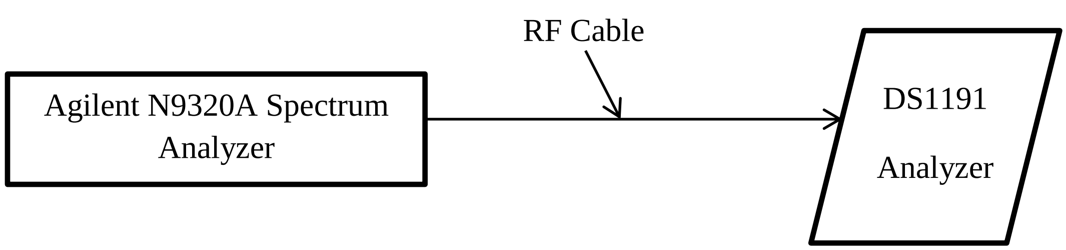

Figure 4.9: Lab Test Model

Transmitter Test Model

We have checked OTV transmitter out before feed to antenna to see the spectrum of modulated signal and received input voltage on DS1191.

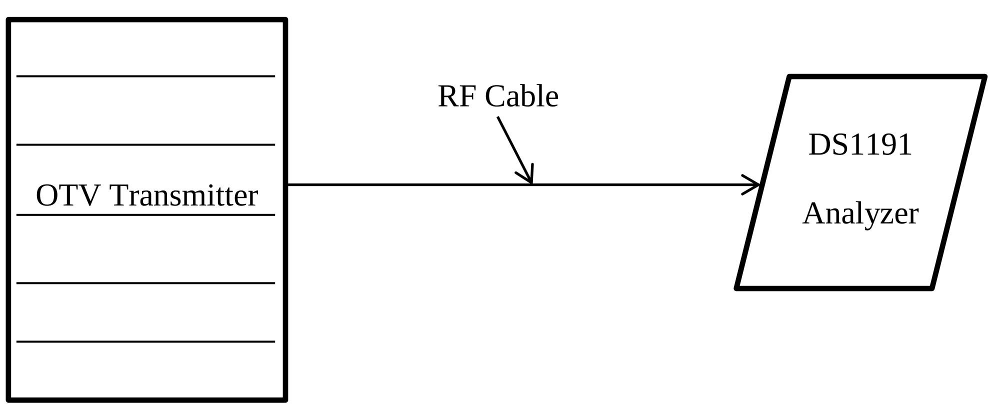

Figure 4.10: Transmitter Test Model

Multipath Reflections Model

We have measured receiver input voltage at different places on the areas affected by multipath reflections i.e. on areas large buildings exist in city centers, wind farm sites, wooded areas open areas of sub-urban and hill's by using dipole antenna, RF cable, DS1191 analyzer and TV sets.

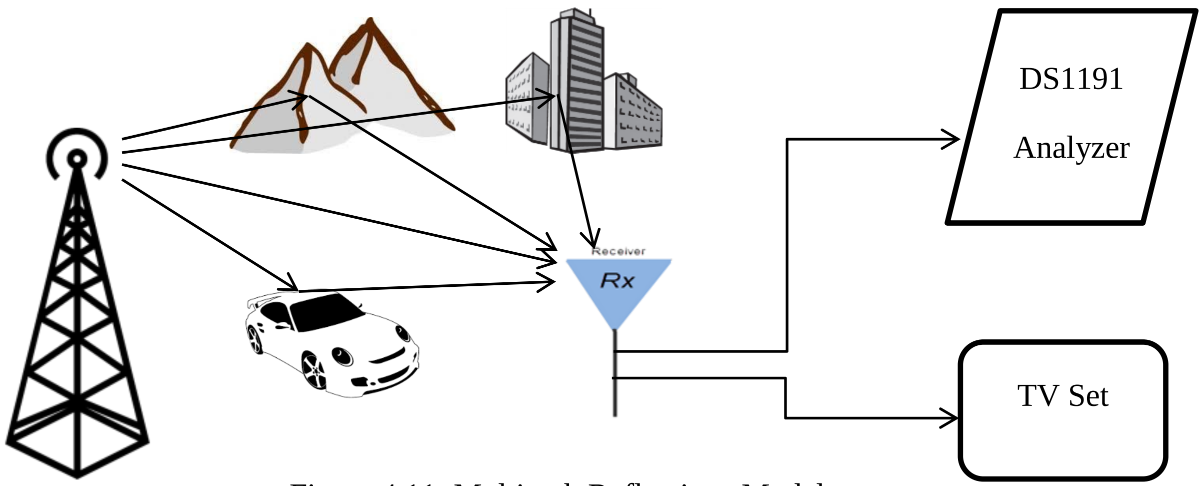

Figure 4.11: Multipath Reflections Model

Co-channel Interference (channel overlaps) Model

We have measured receiver input voltage at different places on the areas affected by co-channel interferences i.e. rays from different transmitters operating at the frequency headed to the receiver at different time or phase angle. By using dipole antenna, RF cable, DS1191 analyzer and TV set.

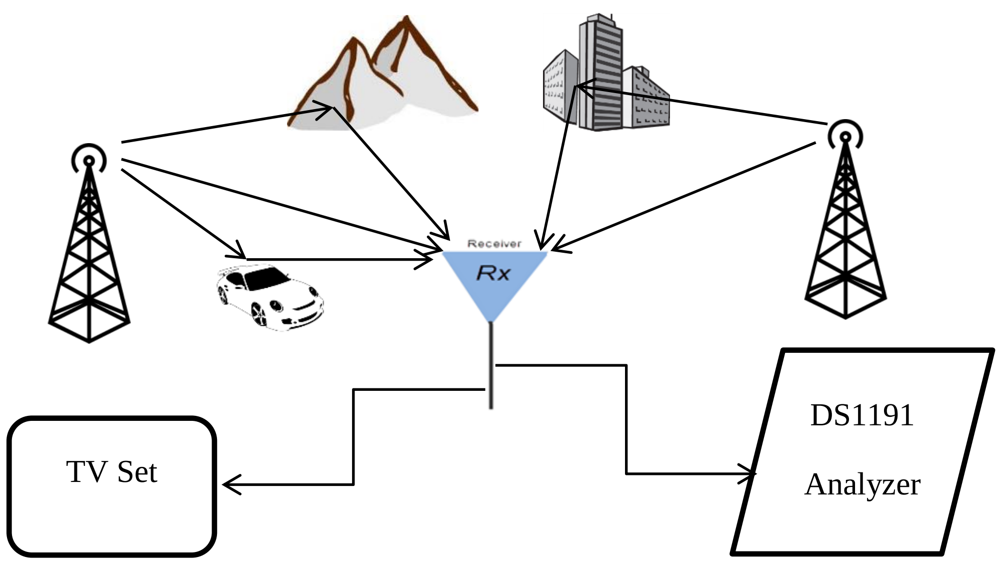

Figure 4.12: Co-channel Interference (channel overlaps) Model

Free Space Propagation Model

We have used friis equation to find the ideal power/input voltage received at an antenna without considering multipath reflections or co-channel interferences (overlaps) by assuming the wave is directly received by receiver in line of sight (LOS) to the transmitter to justify our field measured results.

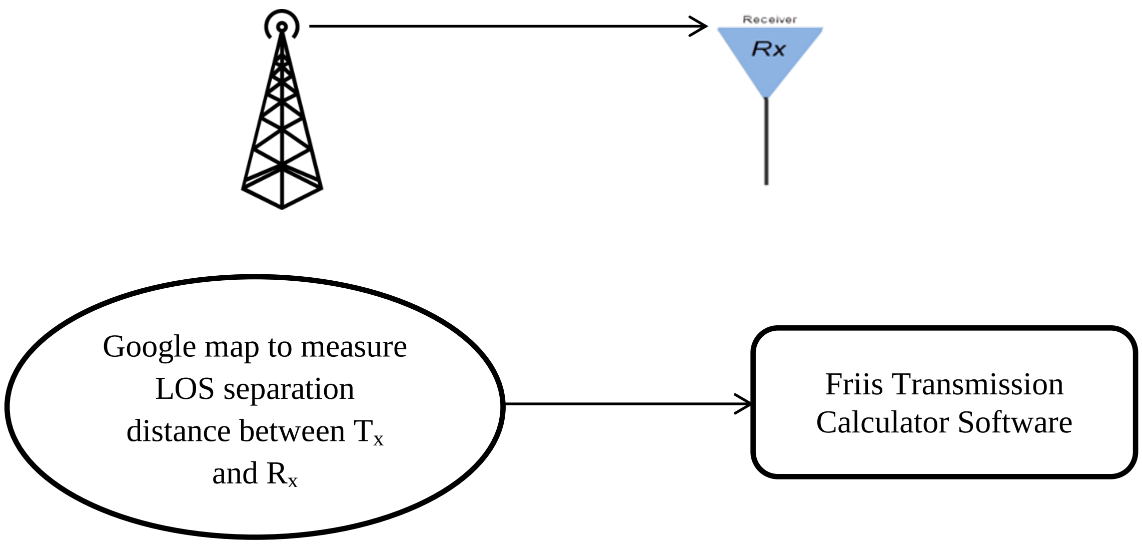

Figure 4.13: Free Space Propagation Model

4.6 Material Used

Agilent N9320A Spectrum Analyzer to generate 10MHz RF

Eurotel VHF terrestrial band III transmitter

DS1191Analyzer to measure receiver input voltage

Dipole Antenna to receive

RF cable

4.7 Software Used

Google Map Developers online distance calculator tool to measure the separation distance between points on the Google maps.

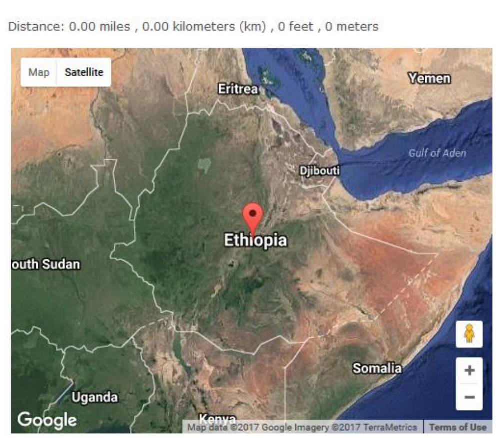

Friis Transmission Calculator is used to find the ideal power received at an antenna from basic information about the transmission.

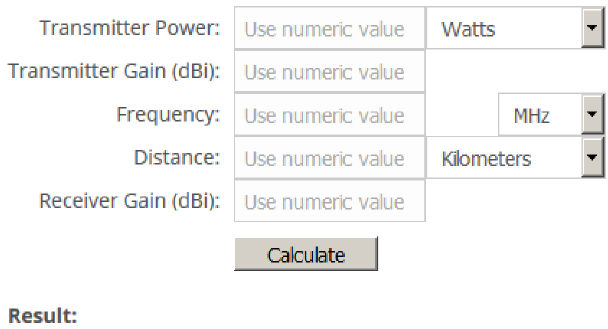

Watts to dBm Conversion Calculator

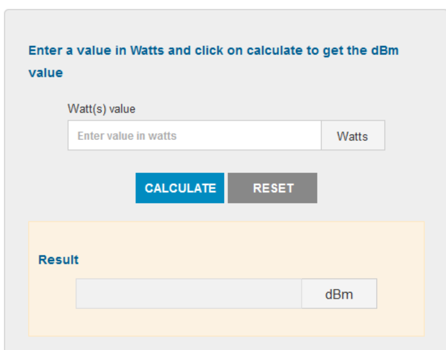

dBm to dBμV Conversion Calculator

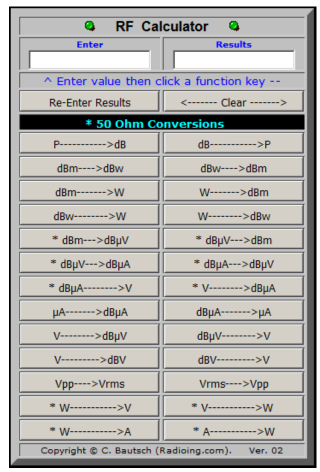

Free Space Path Loss Calculator calculates the loss (in dB) between two antennas where the gain, distance and frequency are known.

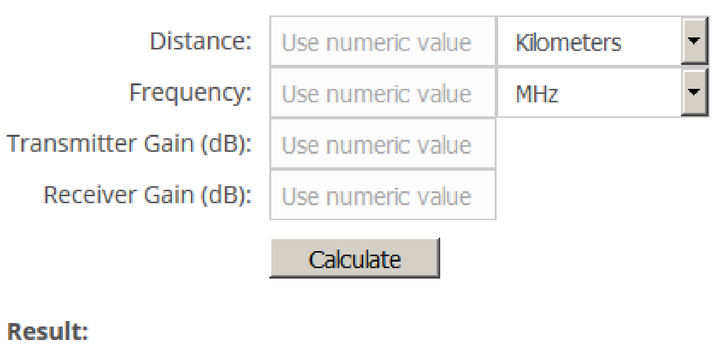

ATDI ICS Telecom is used for simulation of DVB-T guard interval insertions to cancel co-channel overlap or interferences.

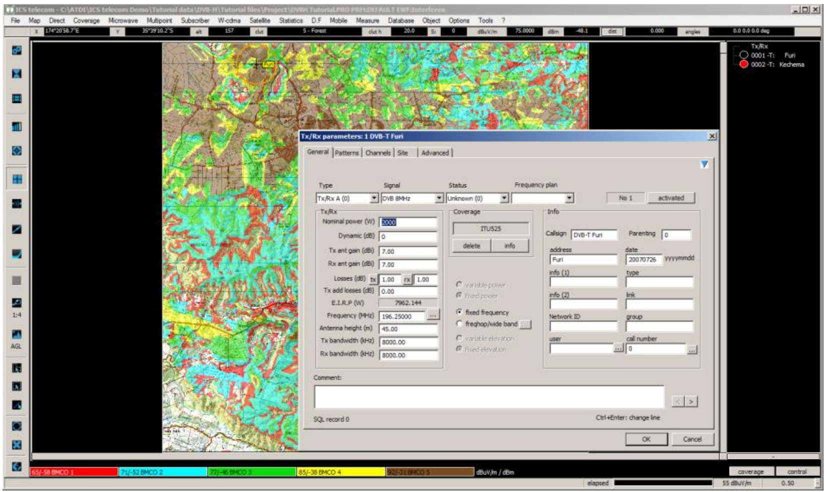

4.8 Parameter Used

We have used parameters of OTV transmitters which are found at adama kechema site and Addis Ababa at furi site.

Parameters (for Adama and Addis Ababa)	**Values**
Frequency of Operation	196.25 MHz
Transmitter Power	2000 Watt
T_x Antenna Height	45 m
R_x Antenna Height	10 m
T_x Antenna Gain	7 dB
R_x Antenna Gain	7 dB
Antenna Pattern	Omni
Adama, Kechema Site Co-ordinates	$8^{0}\ 33'\ 3.61''$ N Latitude
	$39^{0}\ 13'58.11''$ E Longitude
Sabata, Furi Site Co-ordinates	$8^{0}\ 52'\ 56.88''$ N Latitude
	$38^{0}\ 41'12.68''$ E Longitude

Table 4.1: OTV Tx System Parameters

5. Results and Discussions

5.1 Introduction

In this chapter lab test results, field measurement results and simulation results will be presented. In lab test we have measured receiver input voltage and observed spectrum of the Agilent spectrum analyzer and OTV transmitter before the signal fed to transmitter antenna, we have generated 10MHz RF from Agilent spectrum analyzer and also we have used OTV transmitter RF Monitor output and checked on DS1191 analyzer. In field measurements we have measured the receiver input voltage at places where multipath reflections and co-channel overlaps is high. In simulation we have calculated the ideal received power at receiver by measuring line of sight separation distance between transmitter to the receiver by not considering multipath reflections and co-channel overlaps and compared it to field measured results and calculated the path loss between transmitter and receiver by using friis transmission calculator.

5.2 Lab Test

Agilent N9320A Spectrum Analyzer

In the lab we have generated 10MHz RF from Agilent spectrum analyzer and took REF OUT using 15 meter co-axial RF cable and put into DS1191 analyzer RF Input. We have got stable (non-fluctuating) reading of received input voltage in dBµV and clean RF spectrum.

Figure 5.1: Materials used in the Lab

Lab Test Result	
Center Frequency (MHz)	10
Band Width (MHz)	8
Received Input Voltage (dBµV)	70.7

Table 5.1: Lab Test Result

OTV VHF terrestrial band III transmitter

From OTV transmitter which is the operating frequency is 196.25 MHz we have taken REF Monitor Out using RF cable and inserted in DS1191 analyzer RF input. Since REF Monitor Out is a modulated signal and we have got a simple fluctuation in received input voltage amplitude and on spectrum on DS1191 analyzer reading.

Kechema

Furi

Figure 5.2: OTV VHF terrestrial band III transmitter

OTV Transmitter Test Results	
Site	Kechema
Center Frequency (MHz)	196.25
Band Width (MHz)	8
Received Input Voltage (dBμV)	92.6, 93.6, 95.6, 96.0

Table 5.2: Kechem Tx Test Results

OTV Transmitter Test Results	
Site	Furi
Center Frequency (MHz)	196.25
Band Width (MHz)	8
Received Input Voltage (dBμV)	94.9, 95.6, 96.0, 98.1

Table 5.3: Furi Tx Test Results

5.3 Field Measurements

Multi-Path Reflections

We have taken received input voltage measurements in Adama city at different places in the areas multipath reflections is high. We have used 10m dipole antenna, RF cable and DS1191 analyzer to receive OTV signal which is operated at frequency of 196.25MHz. We have pointed or directed our antenna in line of sight (LOS) toward to OTV Transmitter which is found at Adama Kechema site. From these measurements we have got or received multiple input voltages at one place. The reading is not stable it goes up and down in fraction of seconds. These shows multiple rays from different directions and at different phase is receipted by our receiver.

Figure 5.3: Measurement on OTV Building

Specific Place Measured Results	
Place	OTV Building
Center Frequency (MHz)	196.25
Band Width (MHz)	8
Received Input Voltage (dBµV)	27.7, 29.6, 30.6, 33.5, 36.1, 40.6

Table 5.4: Measured Results at OTV Building

As we have seen from the Table 5.4 different rays of OTV signal coming from different direction to our receiving antenna affects the direct signal quality. Since the reflected signal has a delay it was received at different phase. The direct signal geometry was affected destructively. These fluctuations of received input voltage resulted in signal quality degradation and resulted in ghosting effects in our TV sets.

For remaining location at Adama we have registered the fluctuating input voltage result and we have categorized into 3 different values i.e. minimum, average and maximum values. The following Table 5.5 shows these fluctuating input voltages at different places.

Location ID	**Location Name**
1.	OTV Building
2.	AGHMC building
3.	ASTU Front Door Bldg.
4.	Takwa Building 04
5.	Mebrat hayil Emru Bldg.
6.	Posta bet infront of Gadaa
7.	Franko Mamanur Bldg.
8.	Kechema OTV Tx. Site
9.	Adama Wind Farm Site
10.	Open area below kereyu

Table 5.5: Adama Location ID and Name List

Location ID	**Received Input Voltage @ dBμV**		
	Min. Value	***Avg. Value***	***Max. Value***
1.	27.7	35.9625	40.6
2.	30.5	34.825	37.8
3.	31.2	41.29	48.8
4.	31.8	38.918	44.7
5.	30	35.71	43.8
6.	22.3	32.17	38.9
7.	29.4	36.816	42.9
8.	49.8	59.416	68.2
9.	64.4	68.76	77.5
10.	36.5	43.19	50.4

Table 5.6: Received Input Voltage at Adama

In our measurements on OTV building we have connected our antenna out to TV set. In the television screen a pale shadows appear to the right of the original picture which is called the ghosting effect. These effects appear on other places in which we have taken measurements due to long building, structures, trees, wind turbines and moving objects. The phenomena are severe in city centers due large buildings, moving vehicles and poor reflector objects like trees. In city centers the reflected or delayed signals are destructively interrupt the original signal. In areas like wind farms; since the wind turbine blade is metallic it is a good reflector and reflected signal is constructively interrupt the main signal. Figure 5.4 below shows the TV screen shoot at OTV building.

Figure 5.4: Ghost Images on TV Screen from Receiver on OTV Building

Co-Channel Overlaps

We have taken received input voltage measurements at bishoftu city at different places in the areas co-channel overlap is appear. We have used 10m dipole antenna, RF cable and DS1191 analyzer to receive OTV signal which is operated at frequency of 196.25MHz. We have pointed or directed our antenna in line of sight (LOS) toward to OTV Transmitter which is found at Adama Kechema site and Sabata Furi site alternately. From these measurements we have got or received multiple input voltages at one place. The reading is not stable it goes up and down in fraction of seconds and two spectrum appear on our spectrum analyzer screen. These shows OTV signal from kechema and furi at different phase is receipted by our receiver.

Specific Place Measured Results in LOS Kechema Tx	
Place	Four Lakes Market Center
Center Frequency (MHz)	196.25
Band Width (MHz)	8
Received Input Voltage (dBµV)	10.1, 12.0, 13.0, 19, 20.1, 24.0

Table 5.7: Measured Results at 4lake Building in LOS to Kechema

Specific Place Measured Results in LOS Furi Tx	
Place	Four Lakes Market Center
Center Frequency (MHz)	196.25
Band Width (MHz)	8
Received Input Voltage (dBµV)	13.0, 19, 23.4, 27.5, 33.7, 40.1

Table 5.8: Measured Results at 4lake Building in LOS to Furi

As we have seen from the Table 5.7 and 5.8 two rays of OTV signal coming from kechema and furi transmitters received by our antenna in different time. At four lakes market center we have seen signal quality variation when pointing our antenna in LOS of sight to kechema and furi. Whenever we have pointed our antenna towards kechema transmitter the two spectrums values goes down because of kechema is little far away. Whenever we have pointed our antenna towards furi the two spectrums values goes up because of furi is little closer. Since the two signals have a time delay or phase difference between them the main signal is destructively affected. These fluctuations of received input voltage and appearance of the two signals at receiver resulted in signal quality degradation.

For remaining location at Bishoftu we have registered the fluctuating input voltage result and we have categorized into 3 different values i.e. minimum, average and maximum values by pointing our antenna towards Kechema and Furi alternately. The following Tables 5.9 and 5.10 shows these fluctuating input voltages at different places.

Location ID	**Location Name**
1.	Haymanot Building
2.	Four Lakes Market Center
3.	In front of Technic College
4.	Bosena Building
5.	Furi Tx Site

Table 5.9: Bishoftu Location ID and Name List

Location ID	**Received Input Voltage @ dBμV**					
	LOS towards Kechema			***LOS towards Furi***		
	Min. Value	*Avg. Value*	*Max. Value*	*Min. Value*	*Avg. Value*	*Max. Value*
1.	-1.6	4.03	11.7	-9.3	3.58	13.9
2.	10.1	16.38	24	13	26.41	40.1
3.	9.8	17.98	25.7	17.4	24.66	31.7
4.	1.6	9.52	16.4	5.5	14.7	30
5.				65.8	68.8	72

Table 5.10: Received Input Voltage at Bishoftu

From the table above we have observed that OTV signal operated at the same frequency coming from the two transmitters highly affect the received input voltage destructively at receiver because of the phase difference between the two signals. As discussed in chapter 4 the geometry of the ray coming to receiver antenna determines our reception quality.

5.4 Friis Transmission Calculation

Multi-Path Reflections

In Multi-path Reflection environment by using friis transmission calculator we have calculated ideal power received at an antenna from basic information about the transmission in all areas we have taken field measurements. Firstly we have calculated the separation distance between transmitter and receiver by using Google map developer in Adama City. Based on the distance measured and other parameters we have calculated the ideal received input power in watt at a given point and converted it to dBm and dBμV respectively to compare to the measured results. We have also calculated the path loss in dB.

5.5: OTV Transmitter at Adama Kechema Site

5.6 OTV Building

5.7: Separation Distance from OTV to Tx

5.8: Posta Infront of Gada

5.9: Separation Distance from Posta to Tx

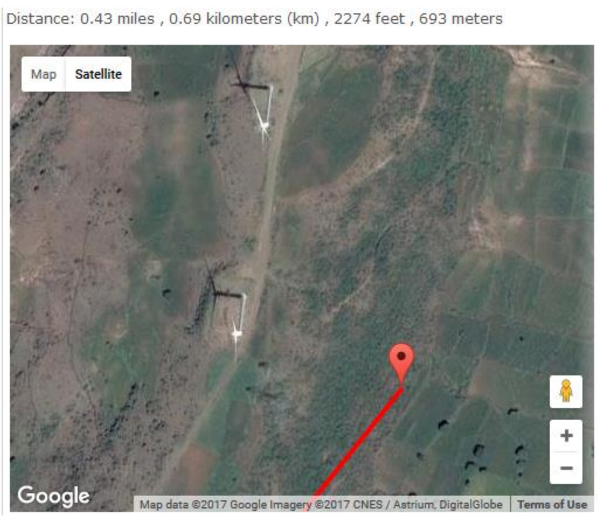

5.10: Wind Farm Site

5.11: Separation Distance from Wind farm to Tx

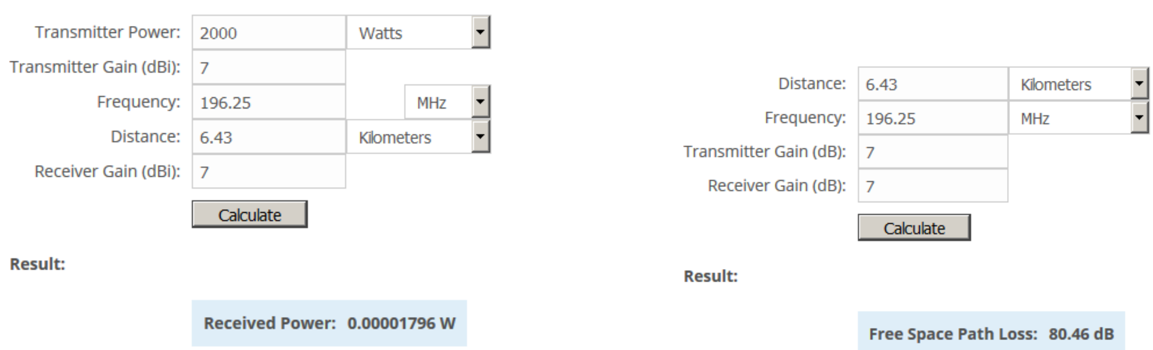

5.12: Ideal Received Power and Free Space Path Loss at OTV Building

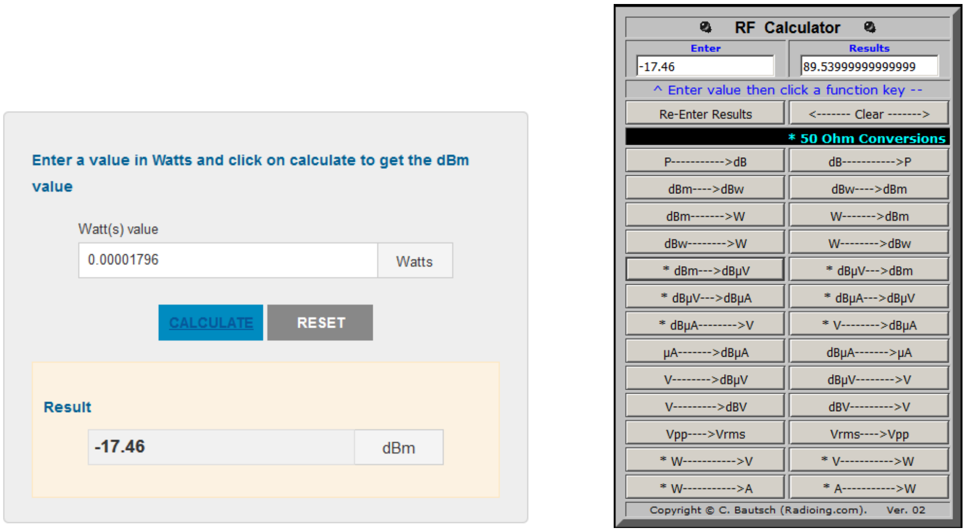

5.13: Ideal Received Power in dBm and dBµV at OTV Building

For remaining places at which measurements took place at Adama we have calculated and listed the ideal received power in the table 5.11 below.

Location Name and ID	Separation Distance	Ideal Received Power			Free Space Path Loss
	Km	Milli Watt	dBm	dBµV	dB
1. TVO Building	6.43	0.01796	-17.46	89.54	80.46
2. AGHMC building	5.6	0.02367	-16.26	90.74	79.26
3. ASTU Front Door Bldg.	5.88	0.02147	-16.68	90.32	79.68
4. Takwa Building 04	4.92	0.03067	-15.13	91.87	78.14
5. Mebrat hayil Emru Bldg.	4.25	0.0441	-13.86	93.14	76.86
6. Posta bet infront of Gada	4.08	0.0446	-13.51	93.49	76.51
7. Franko Mamanur Bldg.	3.6	0.05728	-12.42	94.58	75.42
8. Kechema OTV Tx. Site	0.03	824.29	29.16	136.16	33.84
9. Adama Wind Farm Site	0.69	1.559	1.93	108.93	61.07
10. Open area below kereyu	3.02	0.0814	-10.89	96.11	73.9

Table 5.11: Ideal Received input Power at Adama City

Co-Channel Overlaps

In Co-Channel Overlap environment also we have used friis transmission calculator and calculated ideal power received at an antenna from basic information about the transmission in all areas we have taken field measurements. Firstly we have calculated the separation distance from the two transmitters i.e. Kechema and Furi to our receiver at bishoftu city by using Google map developer. Based on the distance measured and other parameters we have calculated the ideal received input power in watt at a given point and converted it to dBm and dBμV respectively to compare to the measured results. We have also calculated the path loss in dB.

Kechema Site Furi Site

Figure 5.14: OTV Transmitters

Figure 5.15: Four Lakes Market Center

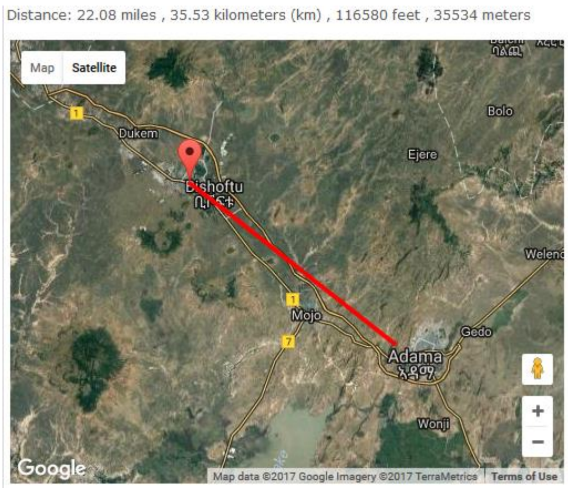

Kechema to 4Lakes

Furi to 4Lakes

Figure 5.16: Separation Distance

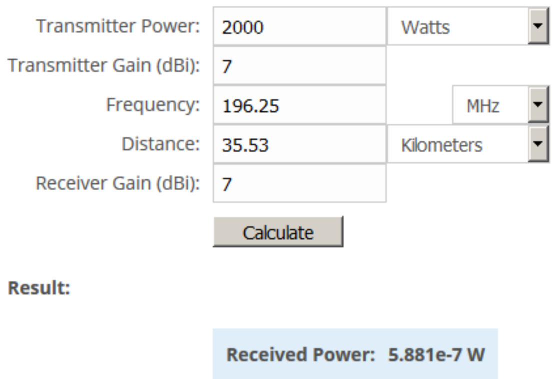

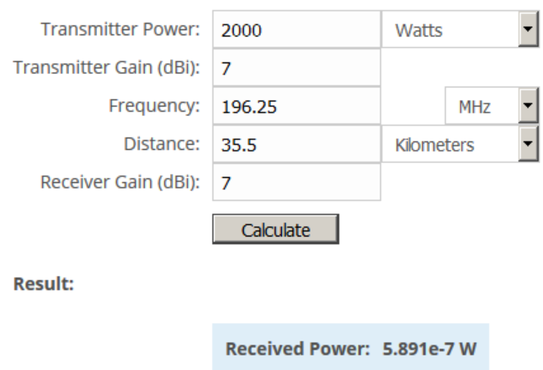

Kechema Parameters

Furi Parameters

Figure 5.17: Ideal Received Power at 4Lakes

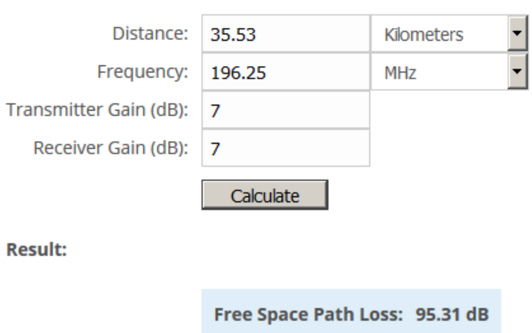

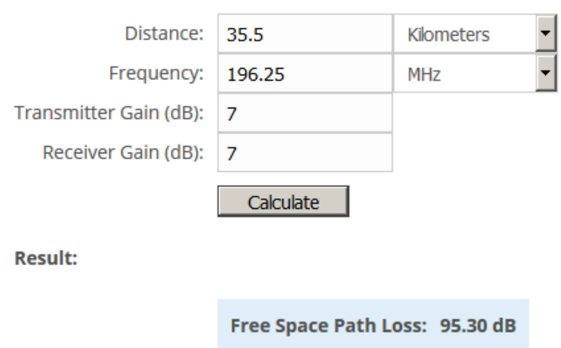

Kechema Parameters

Furi Parameters

Figure 5.18: Free Space Path Loss at 4Lakes

For Bishoftu City we have calculated the ideal received power at all places we have took field measurements and we have also calculated the time difference and phase shift of the OTV signal based on the separation distance between our receiver and the two OTV transmitters. We have used the equation 4.16 which was discussed in chapter 4.

Location Name and ID	Separation Distance (Km)		Time Taken (μs)		Δt (μs)	ϕ^0 (Degrees^0)
	$d_{Kechema}$	d_{Furi}	$t_{Kechema}$	t_{Furi}	t_{Furi} - $t_{Kechema}$	
1. Haymanot Building	33.86	37.2	112.87	124	11.13	94.5^0
2. Four Lakes Market	35.53	35.5	118.43	118.33	0.1	225^0
3. Technic College	37.09	33.81	123.63	112.7	10.93	4.5^0
4. Bosena Building	38.4	32.44	128	108	20	360^0
5. Furi Tx Site		0.03				

Table 5.12: Time difference and Phase Shift

ID	Received Power						Path Loss	
	Kechema			Furi			Kechema	Furi
	Watt	dBm	dBμV	Watt	dBm	dBμV	dB	dB
1.	$6.475e^{-7}$	-31.89	75.11	$5.365e^{-7}$	-32.7	74.3	94.89	95.71
2.	$5.881e^{-7}$	-32.31	74.69	$5.891e^{-7}$	-32.3	74.7	95.31	95.30
3.	5.397e-7	-32.68	74.32	$6.494e^{-7}$	-31.87	75.13	95.68	94.88
4.	$5.035e^{-7}$	-32.98	74.02	$7.055e^{-7}$	-31.52	75.48	95.98	94.52
5.				0.8249	29.16	136.16		33.84

Table 5.13: Ideal Received input Power at Bishoftu City

5.5 Comparison between Measured and Ideal Received Input Voltage

Multi-Path Reflections

In the table 5.14 below we have compared measured receiver input voltage and ideal received input power at the receiver for multipath reflection environment i.e. Adama.

Location Name and ID	**Measured Received Input Voltage (dBµV)**			**Ideal Received Input Voltage (dBµV)**
	Min. Value	***Avg. Value***	***Max. Value***	
1. OTV Building	27.7	35.9625	40.6	89.54
2. AGHMC building	30.5	34.825	37.8	90.74
3. ASTU Front Door Bldg.	31.2	41.29	48.8	90.32
4. Takwa Building 04	31.8	38.918	44.7	91.87
5. Mebrat hayil Emru Bldg.	30	35.71	43.8	93.14
6. Posta bet infront of Gadaa	22.3	32.17	38.9	93.49
7. Franko Mamanur Bldg.	29.4	36.816	42.9	94.58
8. Kechema OTV Tx. Site	49.8	59.416	68.2	136.16
9. Adama Wind Farm Site	64.4	68.76	77.5	108.93
10. Open area below kereyu	36.5	43.19	50.4	96.11

Table 5.14: Comparison of Measured and Ideal Received Input Voltage

Co-Channel Overlaps

For co-channel overlap environments i.e. Bishoftu city we have also compared the measured and ideal received input voltage at receiver see table 5.15 and 5.16 below.

Location Name and ID	**Measured Received Input Voltage (dBµV)**			**Ideal Receive Input Voltage (dBµV)**
	LOS towards Kechema			
	Min. Value	*Avg. Value*	*Max. Value*	
1. Haymanot Building	-1.6	4.03	11.7	75.11
2. Four Lakes Market Center	10.1	16.38	24	74.69
3. In front of Technic College	9.8	17.98	25.7	74.32
4. Bosena Building	1.6	9.52	16.4	74.02

Table 5.15: Comparison of Measured and Ideal Received Input Voltage at Bishoftu in LOS towards Kechema

Location Name and ID	**Measured Received Input Voltage (dBµV)**			**Ideal Receive Input Voltage (dBµV)**
	LOS towards Furi			
	Min. Value	*Avg. Value*	*Max. Value*	
1. Haymanot Building	-9.3	3.58	13.9	74.3
2. Four Lakes Market Center	13	26.41	40.1	74.7
3. In front of Technic College	17.4	24.66	31.7	75.13
4. Bosena Building	5.5	14.7	30	75.48
5. Furi Tx Site	65.8	68.8	72	136.16

Table 5.16: Comparison of Measured and Ideal Received Input Voltage at Bishoftu in LOS towards Furi

5.6 ATDI ICS Telecom Simulation

On the simulation we have inserted DVB-T guard intervals to optimize our network or to reduce interferences caused by co-channel overlaps. We have used the standard parameters as we have used for field measurements.

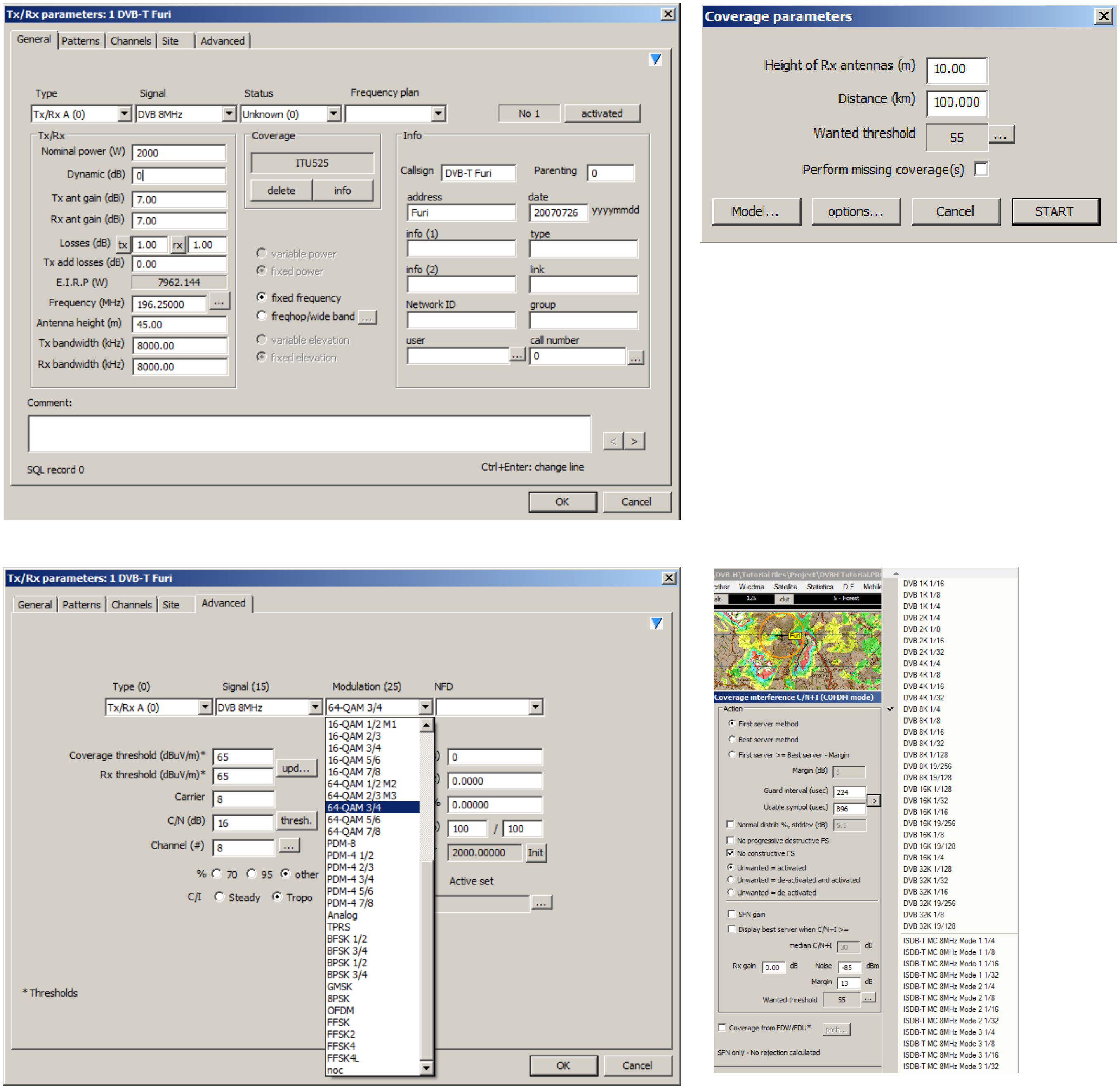

Figure 5.19: Parameters Used for Simulation

Figures 5.20 shows the coverage of two OTV signal transmitted from Kechema and Furi at frequency of 196.25MHz using ics telecom software. The field strength and received input power values of the coverage area indicated in different colors.

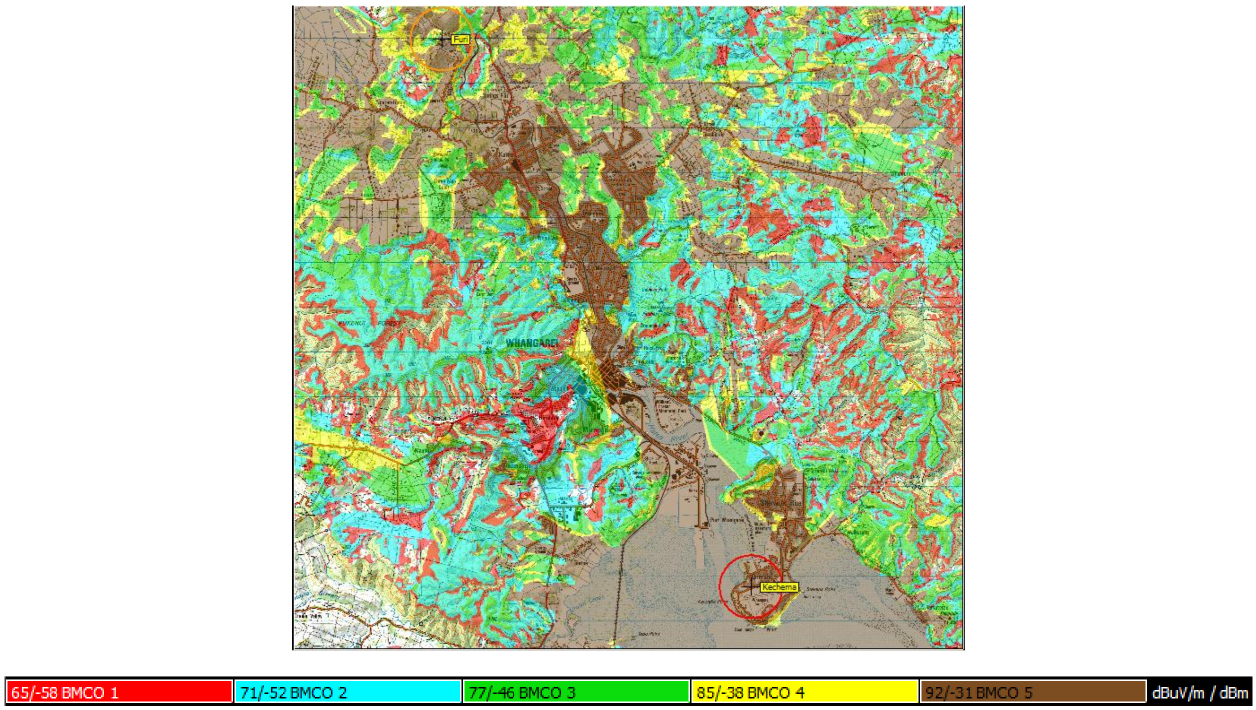

Figure 5.20: Coverage Calculation of Furi and Kechema Transmitters

In the following results we have showed interference cancelling techniques by using different DVB-T guard time. All areas above the minimum threshold (i.e. C/N >=16) indicated in light blue and areas in which there is co-channel overlap or interferences indicated in red. We have simulated for DVB-T 8MHz channel, 64 QAM modulation and 3/4 FEC for 2K and 8k Modes.

DVB-T 8MHz Modulation= 64 QAM FEC= 3/4 for 2K Mode

Guard Interval: 1/32 7 µs

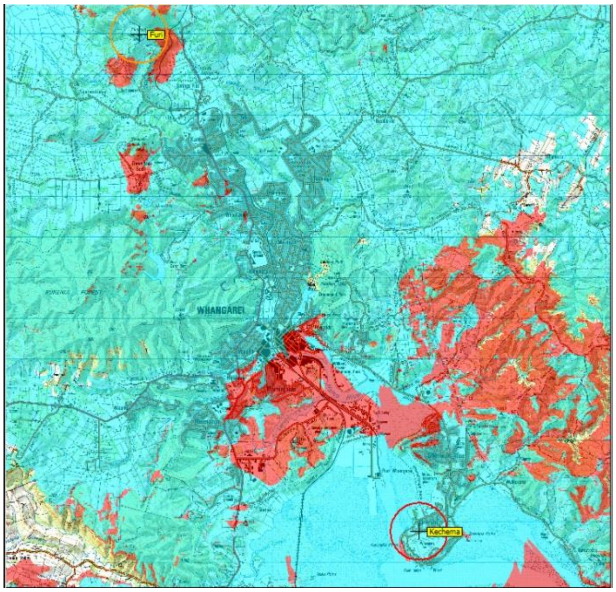

Guard Interval: 1/16 14 µs

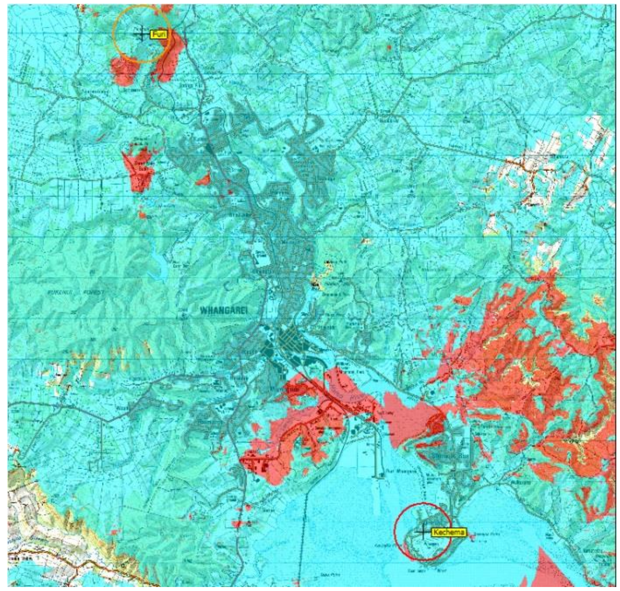

Guard Interval: 1/8 28 µs

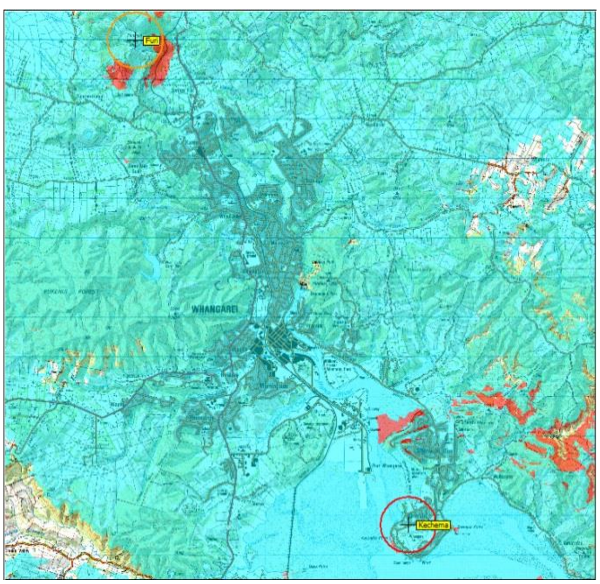

Guard Interval: 1/4 56 µs

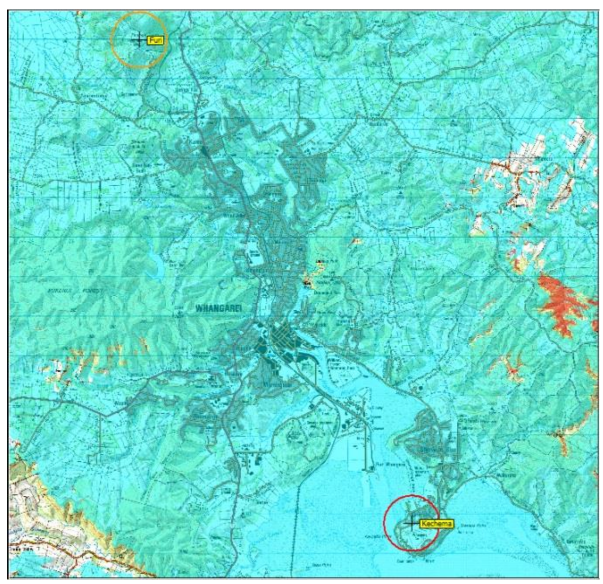

Figure 5.21: DVB-T Guard Insertion for 2k Mode

As shown in the Figure 5.21 for the large guard interval time; interferences are decreasing. For the 2K mode interference is not totally cancelled by the maximum guard interval time.

DVB-T 8MHz Modulation= 64 QAM FEC= 3/4 for 2K Mode Specific Point Analysis

Guard Interval: 1/32 7 µs

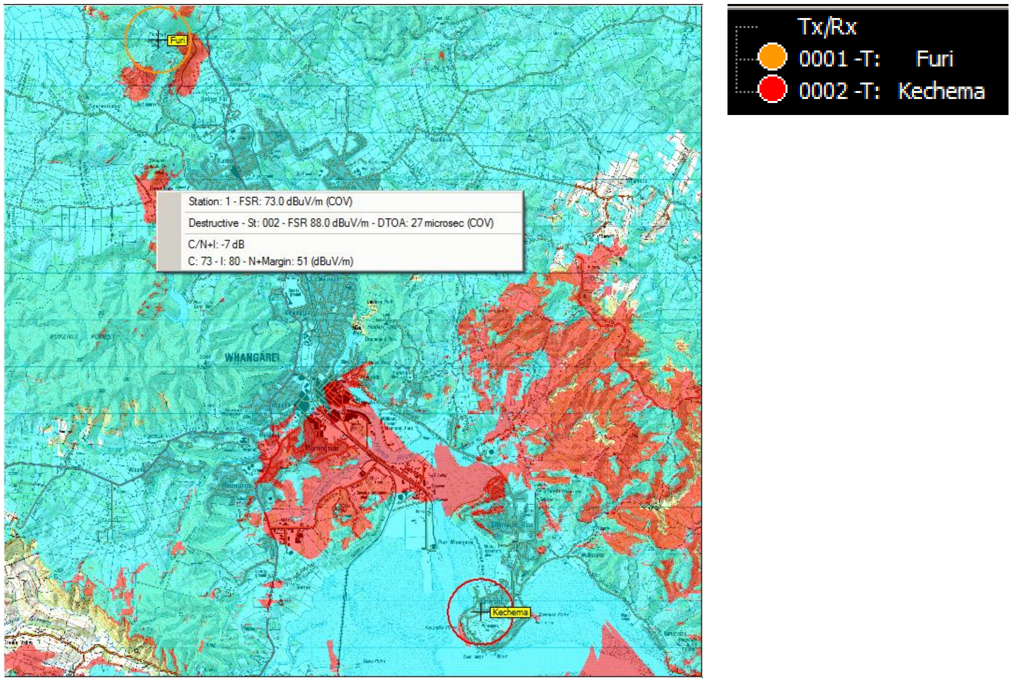

Station 2 is destructively interfering Station 1 reaching at delay of 27 µs. The given guard time is only 7 µs therefore the interference is not faded away in the given guard time.

Guard Interval: 1/16 14 µs

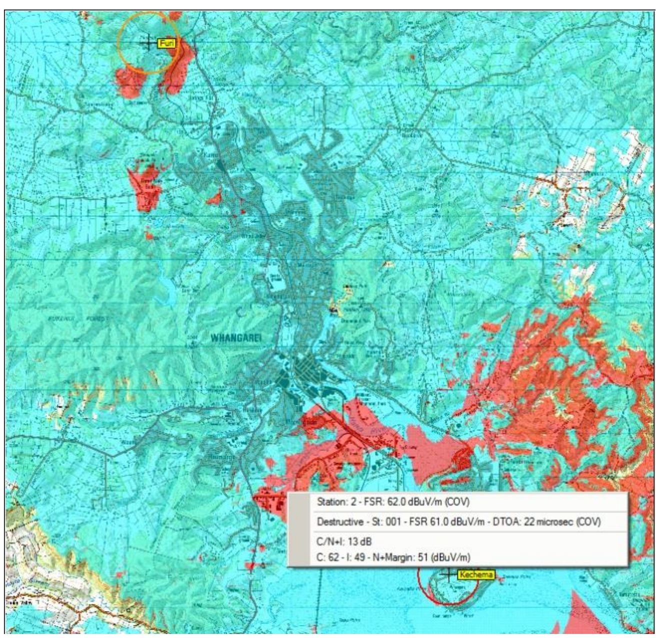

Station 1 is destructively interfering Station 2 reaching at delay of 22 µs. The given guard time is only 14 µs therefore the interference is not faded away in the given guard time.

Guard Interval: 1/8 28 µs

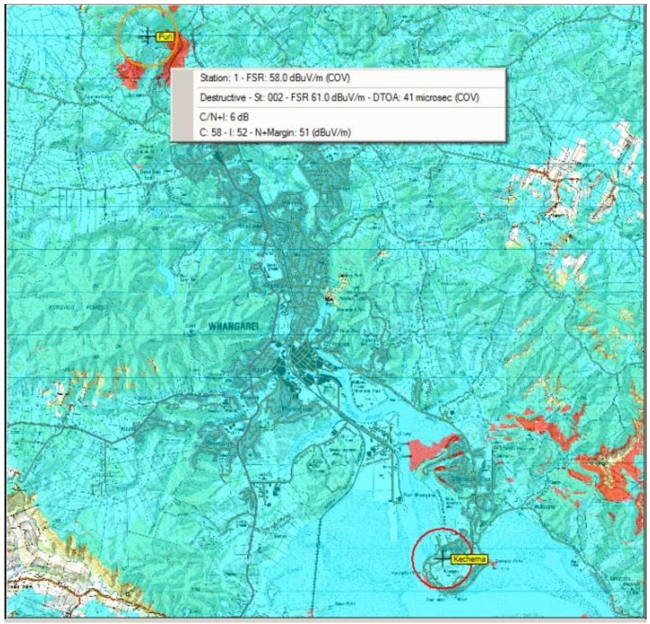

Station 2 is destructively interfering Station 1 reaching at delay of 41 µs. The given guard time is only 28 µs therefore the interference is not faded away in the given guard time.

Guard Interval: 1/4 56 µs

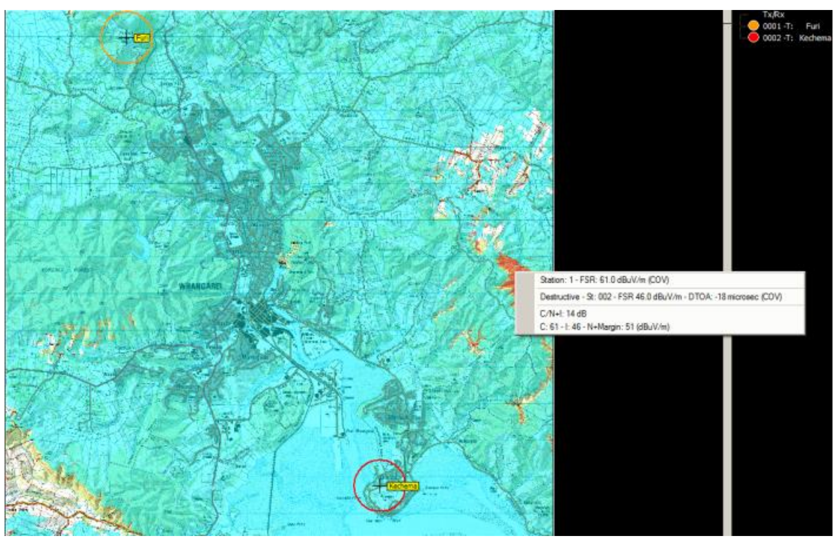

Figure 5.22: Specific Point Analysis for 2k Mode

Station 2 is destructively interfering Station 1 reaching at delay of -18 µs. The given guard time is only 56 µs therefore the interference is not faded away in the given guard time.

From All Figures 5.22 above we have observed that station reaching the receiver of specific point out of the given guard interval/time considered as destructive interferer.

DVB-T 8MHz Modulation= 64 QAM FEC= 3/4 for 8K Mode

Guard Interval: 1/32 28 µs

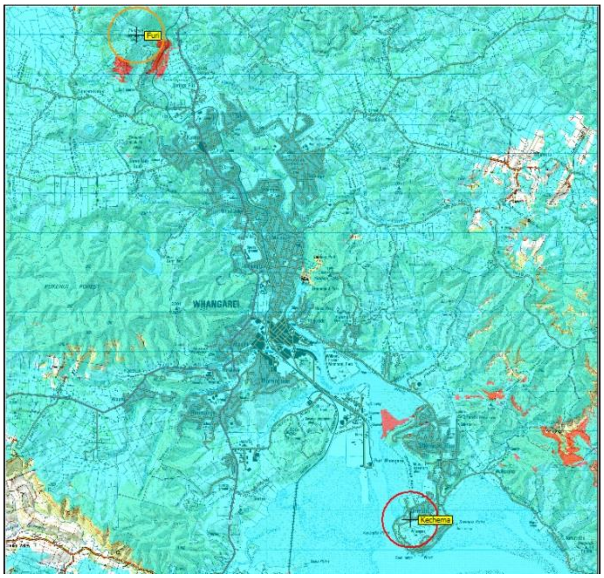

Guard Interval: 1/16 56 µs

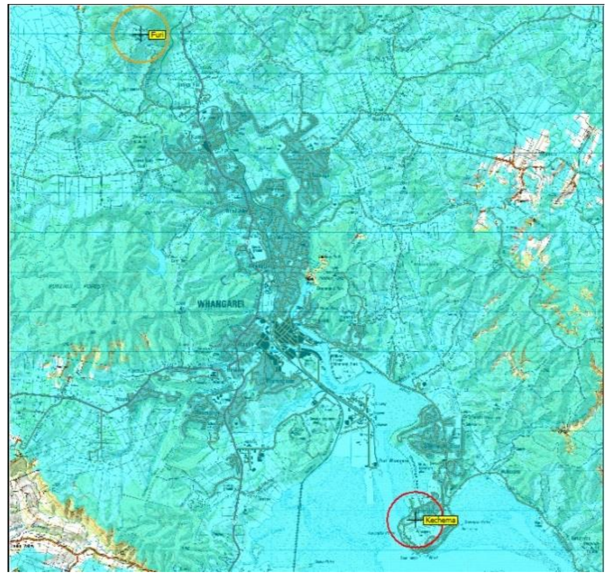

Guard Interval: 1/8 112 µs

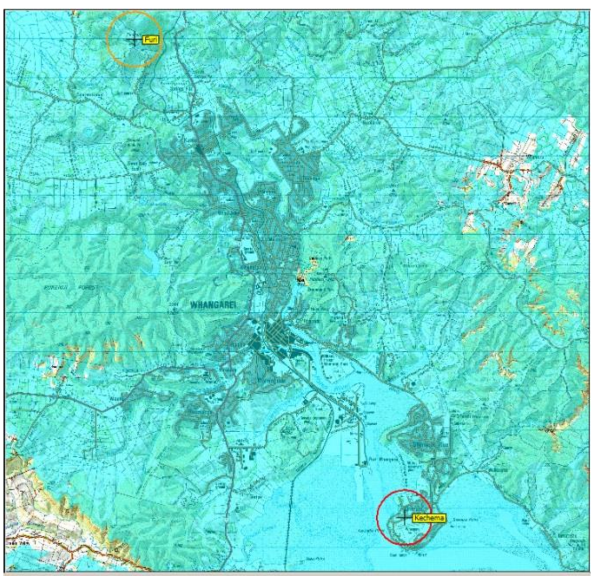

Guard Interval: 1/4 224 µs

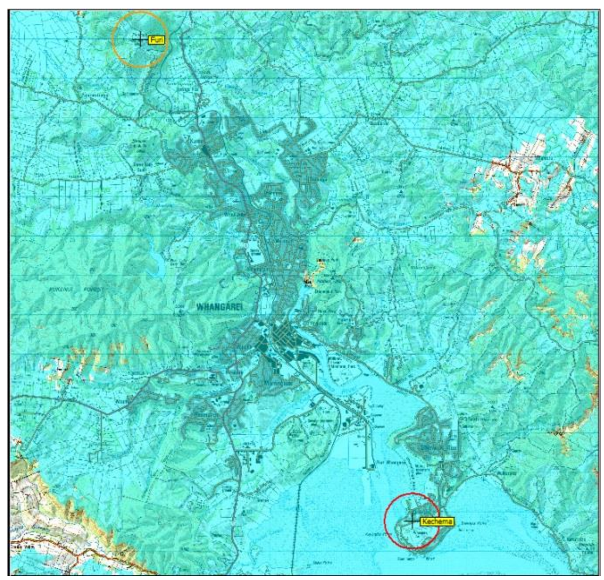

Figure 5.23: DVB-T Guard Insertion for 8k Mode

For 8K mode interference is decreased better than 2k mode. It is eliminated totally at Guard Interval fraction of 1/16 or guards time 56 µs. To better optimize our network we need to have additional FFT size and Guard interval time. Therefore since DVB-T2 has additional FFT sizes, Modulation schemes and Guard interval time or fractions, these interferences will better eliminated totally by introducing DVB-T2. Table below shows improved options of DVB-T2 and the comparison between DVB-T and DVB-T2.

	DVB-T	**DVB-T2** (new/improved options in **bold**)
FEC	Convolutional Coding+Reed Solomon 1/2, 2/3, 3/4, 5/6, 7/8	LDPC + BCH 1/2, **3/5**, 2/3, 3/4, **4/5**, 5/6
Modes	QPSK, 16QAM, 64QAM	QPSK, 16QAM, 64QAM, **256QAM**
Guard Interval	1/4, 1/8, 1/16, 1/32	1/4, **19/128**, 1/8, **19/256**, 1/16, 1/32, **1/128**
FFT Size	2k, 8k	**1k**, 2k, **4k**, 8k, **16k**, **32k**
Scattered Pilots	8% of total	**1%**, **2%**, **4%**, 8% of total
Continual Pilots	2.0% of total	**0.4%-2.4%** (0.4%-0.8% in 8K-32K)
Bandwidth	6, 7, 8 MHz	**1.7**, **5**, 6, 7, 8, **10** MHz
Typical data rate (UK)	24 Mbit/s	**40 Mbit/s**
Max. data rate (@20 dB C/N)	31.7 Mbit/s (using 8 MHz)	**45.5 Mbit/s** (using 8 MHz)
Required C/N ratio (@24 Mbit/s)	16.7 dB	**10.8 dB**

Table 5.17: Comparison of DVB-T and DVB-T2

DVB-T 8MHz Modulation= 64 QAM FEC= 3/4 for 8K Mode Specific Point Analysis

Guard Interval: 1/32   28 µs

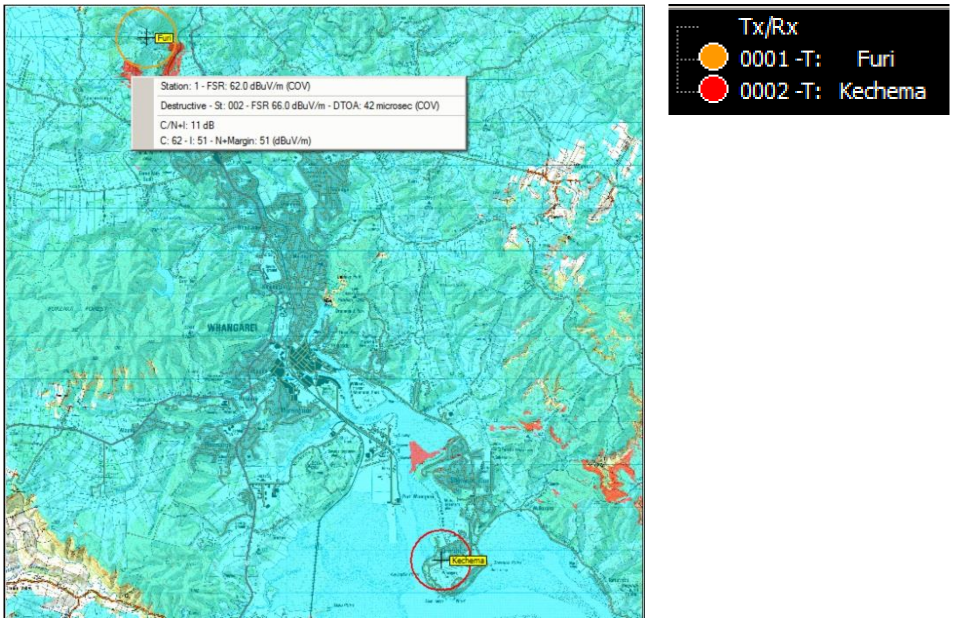

Station 2 is destructively interfering Station 1 reaching at delay of 42 µs. The given guard time is only 28 µs therefore the interference is not faded away in the given guard time. But interferences reduced in 8k Mode better than 2k Mode.

Guard Interval: 1/16   56 µs

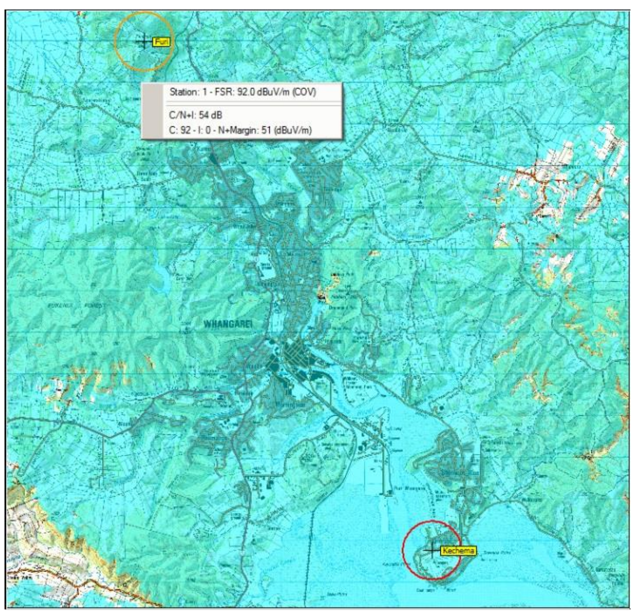

On the specific point only Station 1 is reaching. There is no destructive interference in our network. All delayed signals faded in the given guard time i.e. 56 µs for DVB-T 8 MHz 8K Mode.

Guard Interval: 1/8   112 µs

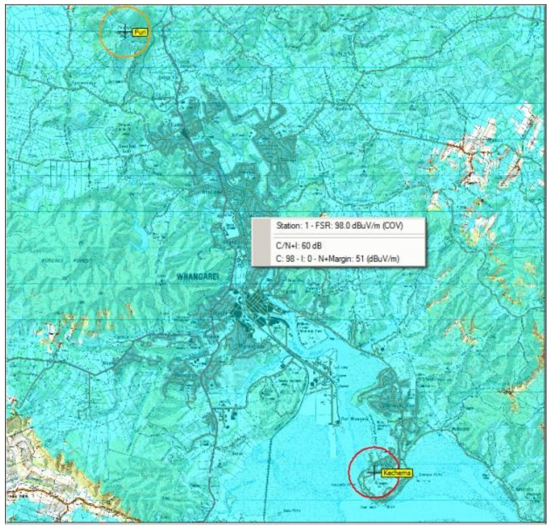

On the specific point only Station 1 is reaching. There is no destructive interference in our network. All delayed signals faded in the given guard time i.e. 112 µs for DVB-T 8 MHz 8K Mode.

Guard Interval: 1/4   224 µs

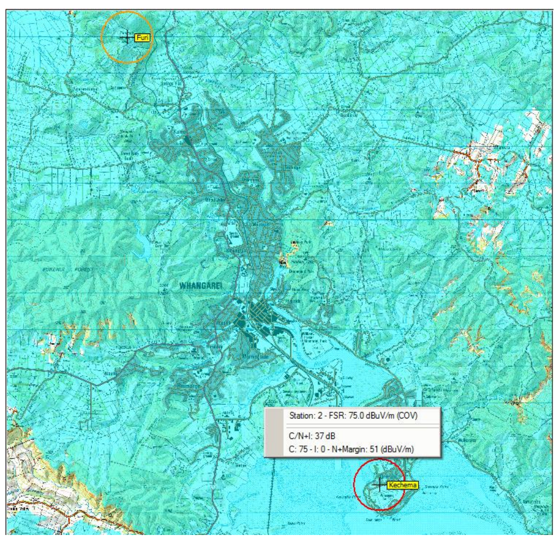

Figure 5.24: DVB-T Guard Insertion for 8k Mode

On the specific point only Station 2 is reaching. There is no destructive interference in our network. All delayed signals faded in the given guard time i.e. 224 µs for DVB-T 8 MHz 8K Mode.

As we have seen from All Figures of 5.24 above all interferences are faded away at 56 µs guard time for DVB-T 8 MHz 8k Mode. Our network is optimized and able to deliver qualified signal.

6. Conclusion and Recommendation

6.1 Conclusion

Reflected or delayed analog OTV signal affects the quality of main or required signal. In developing cities like Adama in which long buildings, wind turbines, trees, structures and vehicles are appearing the effect of ghosting is too high. Since reflected signals took longer path it reaches the receiver later than the main signal. These phenomena leads to the phase shift of two or more signals operating at the same frequency. Due to these constructive or destructive interferences happened to the main signal depending on the property of the reflector body. Metallic objects like wind turbines are good reflector and delay is too short. Objects like trees are poor reflector and delay is high which leads to destructive interferences.

OTV signal coming from two transmitters operating at the same frequency affects the received signal quality. In cities like Bishoftu in which OTV signals are reaching the receiver from the two transmitters are seriously affected. In some places of Bishoftu city the two signals are totally cancel each other.

Because of multi-path reflections and co-channel overlaps the required input voltage is not reaching the receiver and leads to reduced picture quality or ghost images on our TV sets.

Co-channel overlaps or interferences could be eliminated by inserting proper guard intervals which helps us to optimize our network to deliver qualified audio and video signals.

6.2 Recommendation

In terrestrial broadcasting (Analog or Digital) reflections (echoes) will be produced during the transmission, in DTT the pause times called guard intervals will enable these echoes to fade away and do not affect the signal reception. This will allow extinguishment of echoes or reflections of the transmitted signal, or signals from other co-channel transmission of the same network reaching the receiver with a certain delay. The longer the guard interval, the greater the time allowed to extinguish unwanted echoes, but the lower the quantity of data that can be transmitted (bit-rate – number and/or quality of programs). We recommend the Oromia Radio and TV Organization (ORTO) to migrate to DVB-T2 to avoid interferences caused by multipath reflections and co-channel overlaps. Since For DVB-T2, the range of standard COFDM parameters has been extended compared with DVB-T.

Since the separation distance between our two transmitters over air (i.e. Furi and Kechema) is 70.52 km apart. We recommend DVB-T2 256 QAM, 32k Mode, adequate FEC 3/4 and Guard fraction of 19/256 or guards time 266 µs with data rate of 42.998 Mbit/s while launching DVB-T2 SFN, because in this guard time delayed signal coming from up to 79.9km will be synchronized.

To better receive DVB-T2 signals for Transmitter operating at 2000W:

For the transmitter 15km away to the receiver we shall use Indoor DVB-T/T2 Antenna with Amplifier with gain of 21dB.

For the transmitter between 15km and 40km away to the receiver we shall use Outdoor DVB-T/T2 Antenna (log periodic) with gain of 8/9dBi.

For the transmitter above 40km away to the receiver we shall use Outdoor UHF TV Antenna: DIPOL 16/21-60 with LNA-177 Amp; with gain of 42dB.

References

1. Second Generation Terrestrial, The World's Digital Terrestrial TV Standard, DVB Fact Sheet - August 2016.
2. What is Guard Interval in DVB-T and DVB-T2 systems? (22-mar-2017). Retrieved from http://www.satbroadcasts.com/news,83,What_is_Guard_Interval_in_DVB_T_and_DVB_T2_systems.html
3. Terrestrial television reception disturbances, Leszek AUGUSTYNIAK, Bialystok University of Technology Faculty of Electrical Engineering
4. Report ITU-R BT.2140-7 (04/2014), Transition from analogue to digital terrestrial broadcasting, BT Series Broadcasting service (television).
5. Tech 3348, Frequency and Network Planning Aspects of DVB-T2, Status: Report, Version 4.1.1 Geneva October 2014.
6. OFCOM, Tall structures and their impact on broadcast and other wireless services, 26 August 2009.
7. Recommendation ITU-R Bt.1124-2, Reference Signals For Ghost Cancelling In Analogue Television Systems, (Question ITU-R 55/11) (1994-1995-1998).
8. Digital Terrestrial Television Broadcasting: Technology and System; Wiley.
9. Single Frequency Networks For Digital Video Broadcasting, by JM Fernández, J Capdevila, R García, S. Cabanillas, S Mata, A Mansilla and JM Fernández Engineering R&D - RETEVISION S.A., Spain.
10. Google Map Developers (26-Apr-2017). Retrieved from https://www.mapdevelopers.com/distance_finder.php
11. Friis Transmission Calculator (26-Apr-2017). Retrieved from https://www.pasternack.com/t-calculator-friis.aspx
12. Watts to dBm Conversion Calculator (26-Apr-2017). Retrieved from https://www.everythingrf.com/rf-calculators/watt-to-dbm
13. e Engineer ~ Virtual Tools (26-Apr-2017). Retrieved from http://www.radioing.com/eengineer/rfcalc.html
14. Free Space Path Loss Calculator (26-Apr-2017). Retrieved from https://www.pasternack.com/t-calculator-fspl.aspx
15. Phase in Acoustics (27-Apr-2017). Retrieved from http://www.sengpielaudio.com/calculator-timedelayphase.htm
16. Ghost Cancelling And Cable Nick Hamilton-Piercy And Gary Chan Rogers American Cablesystems Inc.

17. Artefacts in Image and Video Systems: Classification and Mitigation, Amal Punchihewa and Donald G. Bailey Institute of Information Sciences & Technology, Massey University g.a.punchihewa@massey.ac.nz d.g.bailey@massey.ac.nz.
18. GREENBERG, C. B. 1993. Ghost Cancellation System for the US standard GCR, IEEE Transaction on Consumer Electronics, 39(4) 928-933.
19. CHINI, A., WU, Y., TANANY, EL- T., AND MOHMOUD, S. 1998. Filter Decision Feedback channel Estimation for OFDM based DTV Terrestrial Broadcasting System. IEEE Transaction on Broadcasting, 44(1) 2-11.
20. JEON, B., AND JEONG, J. 1998. Blocking Artifacts Reduction in Image Compression with Block Boundary Discontinuity Criterion, IEEE Transaction on Circuits and Systems, 8(3) 345-357.
21. HUANG, J. 1993. A Ghost Cancellation System for the NTSC Television", IEEE Transaction on Consumer Electronics, 39(4) 896-904.
22. APPELHANS P., AND SCHRODER, H. 1995. Ghost Cancelling for Stationary and Mobile Television, IEEE Transaction on Consumer Electronics, 41(3) 472-786.
23. AL-SAUD, W.A.A., EL-HENNAWEY, M. S. AND BORAIE, M.T. 1996. A New GCR Waveform for Deghosting TV Signals, IEEE Transaction on Consumer Electronics, 42(4) 920-929.
24. FIALLOS, E., HARMASZ, J., CARON, B., AND LEDOUX, B. 1994, An enhanced Ghost Cancellation Reference Signal, IEEE Transaction on Consumer Electronics, 40(3) 640-644.
25. YANG, K. S., PARK, H. M., PARK, J. H., AND KIM, K. B. 1994. A New GCR Signal and its Application, IEEE Transaction on Consumer Electronics, 40(4) 852-860.
26. GUNTURK, B.K., LTUNBASAK, Y.A., AND MERSEREAU, R.M. 2000. Multiframe Blocking-Artifact Reduction for Transform-Coded Video, IEEE Transaction on Circuits and Systems, 12(4) 276-282. Report ITU-R BT.2254-1 (11/2013), Frequency and network planning aspects of DVB-T2, BT Series Broadcasting service (television).
27. PATTI, A.J., AND ALTUNBASAK, Y. 2001. Artifact Reduction for Set Theoretic Super Resolution Image Reconstruction with Edge Adaptive Constraints and Higher-Order Interpolants, IEEE Transaction on Image Processing, 10(1) 179-186.
28. JEONG, Y., KIM, I., AND KANG, H. 2000 A Practical Projection- Based Postprocessing of Block-Coded Images with Fast Convergence Rate, IEEE Transaction of Circuits and Systems, 10(4) 617-623.
29. LIU, C., WANG C., AND LIN, J. 1998. A New Postprocessing Method for the Block-Based DCT Coding Based on the Convex-Projection Theory, IEEE Transaction on Consumer Electronics, 44(3) 1054-1061.

30. PAEK, H., KIM, R., ANDLEE S. 1998. On the POCS-Based Postprocessing Technique to Reduce the Blocking Artifacts in Transform Coded Images. IEEE Transaction on Circuits and Systems for Video Technology, 8(3) 358-367.
31. KIM, Y., JUNG, J., CHOI, K., AND KO, S. 2001. Post-Processing Technique Based on POCS for Visual Enhancement in HDTV Images, IEEE Transaction on Consumer Electronics, 47(3) 652-659.
32. MEIER, T., NGAN, K.N., AND CREBBIN, G. 1999. Reduction of Blocking Artifacts in Image and Video Coding, IEEE Transaction on Circuits and Systems, 9(3) 490-500.
33. ROBERTSON, M.A., AND STEVENSON, R. L. 2001 Reduced- Complexity Iterative Post-Filtering of Video. IEEE Transaction on Circuits and Systems. 11(10) 1121-1127.
34. WANG, Z., AND ZHANG, D. 1998. A Novel Approach for Reduction of Blocking Effects in Low-Bit-Rate Image Compression, IEEE Transaction on Communications, 46(6) 732-734.
35. CAO, Y., EGGERMONG, P.P.B., AND TEREBY, S. 1999. Cross Burg Entropy Maximization and Its Application to Ringing Suppression in Image Reconstruction, IEEE Transaction on Image Processing, 8(2) 286-292.
36. MATEOS, J., KATSAGGELOS, A. K., AND MOLINA, R. 2000. A Bayesian Approach for the Estimation and Transmission of Regularization Parameters for Reducing Blocking Artifacts, IEEE Transaction on Image Processing, 9(7) 1200-1215.
37. ATZORI, L., NATALE, F.G.B., AND DE PERRA, C. 2001. A Spatio- Temporal Concealment Technique Using Boundary Matching Algorithm and Mesh-Based Wraping (BMA-MBW), IEEE Transaction on Multimedia, 3(3), 326-338.
38. QUI, G. 2000. MLP for Adaptive Postprocessing Block-Coded Images, IEEE Transaction on Circuits and Systems, 10(8) 1450-1454.
39. MEXTREAM FRANCE (A joint venture of Alcatel and Thomson Multimedia) 2001. Technical Report on Superencoder.
40. CARLI, M., BAILEY, D., FARIAS, M., AND MITRA, S. K. 2002. Error control and concealment for video transmission using data hiding, International symposium on wireless personal multimedia communications.
41. HSUNG, T., AND LUN, D.P. 1998. Application of Singularity Detection for the De blocking of JPEG Decoded Images, IEEE Transaction on Circuits and Systems-II: Analogue and Digital Signal Processing, 45(5) 640–644.
42. MALVAR, H.S. 1998. Biorthogonal and Nouniform Lapped Transforms for Transform Coding with Reduced Blocking and Ringing Artifacts, IEEE Transaction on Signal Processing, 46(4) 1043-1053.
43. CAREY, W. K., HAMAMI, S.S., AND HELLER, P.N. 1999 Smoothness-Constrained Quantization for Wavelet Image Compression, IEEE Transaction on Image Procrocessing, 8(12) 1807-1811.

44. DUBUC, C., BOUDREAU D., AND PATENAUDE, F. 2001. The Design and Simulated Performance of a Mobile Video Telephony Application for Satellite Third-Generation Wireless System, IEEE Transaction on Multimedia, 3(4) 424-431.
45. CHANG, Y., CARNEY, T., KLEIN, S. A., MESSERSCHMITT, D. G., AND ZAKHO, A. 1998. Effects of Temporal Jitter on Video Quality: Assessment Using Psychophysical Methods, Proceedings of the SPIE: Human Vision and Image Processing.
46. Report ITU-R BT.2254-1 (11/2013), Frequency and network planning aspects of DVB-T2, BT Series Broadcasting service (television).
47. Application Note, Understanding Single Frequency Network Measurements, MS2721B Spectrum Master, MS2712E/MS2713E Spectrum Master, MT8212E/MT8213E Cell Master.
48. Report ITU-R BT.2386-0 (07/2015), Digital terrestrial broadcasting: Design and implementation of single frequency networks (SFN), BT Series Broadcasting service (television).
49. Single Frequency Networks (SFN) in Digital Terrestrial Broadcasting, Václav ŘÍČNÝ Dept. of Radio Electronics, Brno University of Technology, Purkyňova 118, 612 00 Brno, Czech Republic, ricny@feec.vutbr.cz.
50. Single Frequency Networks for DVB-T and Evolution towards DVB-T2, Sanja Maksimović - Moićević1), Danijela Šikanja - Marković2), Željen Trpovski3).